Global Nonlinear Solutions in Sequence Space and the Generalized Transition Function[*]

Hanbaek Lee[†]

University of Cambridge

April 8, 2025

Abstract

This paper develops a unified framework for globally solving dynamic stochastic general equilibrium models with high accuracy and computational efficiency in sequence space. The method efficiently handles rich heterogeneity, nonlinearities such as occasionally binding constraints, and non-trivial market clearing conditions — without assuming perfect foresight. Building on this, I introduce the generalized transition function (GTF), defined as a sub-path of the recursive competitive equilibrium. The GTF nests generalized impulse responses and stochastic growth paths, enabling global analysis of state-dependent dynamics and the interaction between growth and uncertainty. Applications to heterogeneous-agent models with occasionally binding constraints and portfolio choice reveal rich equilibrium predictions driven by the cross-sectional heterogeneity — including uncertainty-driven dampened growth, endogenous disasters, state-dependent fiscal multipliers, heterogeneous portfolio adjustments over the business cycle, and state-dependent risk premium dynamics.

Keywords: Global nonlinear solution, sequence space, generalized transition function, heterogeneous agents.

JEL codes: C63, E32, E21

---

1 Introduction

Modern macroeconomic analysis faces a critical challenge: real-world economies exhibit rich heterogeneity and complex nonlinearities that our analytical tools struggle to capture fully. This methodological gap has limited capacity to answer fundamental questions in economics including how growth interacts with uncertainty, what drives recessions, and when a policy can effectively intervene.

This paper fills this gap through three key contributions. First, it develops a powerful global nonlinear solution framework in the sequence space. It does not assume perfect foresight, efficiently handles occasionally-binding constraints, and computes state-contingent expectations without parameterizing laws of motion. The framework provides a substantial computation gain for models with period-by-period fixed-point problems such as non-trivial market clearing conditions—accelerating the computation of heterogeneous models by more than tenfold. This advancement enables efficient solutions to computationally challenging problems that were considered prohibitively expensive to solve, including heterogeneous-agent models with multiple non-trivial market clearing conditions, as demonstrated in the applications. Moreover, it provides theoretical foundations for using sufficient statistics to solve dynamic stochastic general equilibrium (DSGE, hereafter) models with rich heterogeneity. This theoretical advance enables the method to efficiently solve a broad spectrum of macroeconomic models – from a standard representative-agent real business cycle model to cutting-edge heterogeneous-agent models with multidimensional aggregate states – all within a unified simple computational framework.[1]

Second, this paper introduces a generalized transition function (GTF), which captures short-run stochastic equilibrium dynamics over any possible exogenous state paths. Each GTF is a sub-path of the recursive competitive equilibrium (RCE), which nests generalized impulse response functions (GIRF) (Koop et al., 1996; Andreasen et al., 2017) and stochastic growth path (Justiniano and Primiceri, 2008; Hansen et al., 2008). The generalized transition function (GTF) provides a critical theoretical bridge between abstract RCE and practical analysis of nonlinear, state-dependent macroeconomic dynamics. While RCE offers a powerful conceptual framework, it has traditionally been difficult to leverage this object for analyzing complex transitions between different states or history-dependent paths. The GTF addresses this gap by formalizing transition dynamics as a sub-path of the standard recursive competitive equilibrium, enabling rigorous analysis of stochastic transitions

---

[1]More than 20 sample MATLAB codes for various DSGE models with representative or heterogeneous agents (households/firms), various frictions, occasionally binding constraints, multiple aggregate states, New Keynesian, or DMP are available at https://sites.google.com/view/hanbaeklee/computation-lab?authuser=0.

within an integrated equilibrium framework. The global solution of this paper immediately computes the GTF as it's a part of the RCE. The GTF opens the door to two relatively under-explored macroeconomic research topics: 1) endogenous interaction between the growth and the business cycle components through the short-run stochastic growth path and 2) the state-dependent shock responsiveness of economic variables on the RCE, obviating the need for analyses based on different steady states.

Third, beyond its methodological contributions, the framework delivers several substantive economic insights that are inaccessible to standard solution methods. These emerge from applications of the integrated RCE framework to two heterogeneous-household RBC models: (1) one with endogenous labor supply, investment irreversibility, and fiscal spending shocks, and (2) another with portfolio choice and endogenous labor supply. There are five key takeaways. First, the economy displays endogenous fragility: when a larger share of households are hand-to-mouth, moderate shocks generate disproportionately severe downturns. This helps explain why similar exogenous shocks can produce dramatically different outcomes across time. Second, uncertainty dampens short-run growth when capital adjustment is subject to irreversibility. This highlights a novel interaction between uncertainty and growth that is typically overlooked in macro models. Third, fiscal multipliers vary strongly with the distribution of hand-to-mouth households, confirming the mechanism in Kaplan and Violante (2014) within the fully nonlinear RCE framework. Fourth, portfolio adjustment differs starkly across the wealth distribution: wealth-poor households maintain highly leveraged risky positions and rebalance aggressively over the business cycle, frequently hitting borrowing constraints—unlike wealth-rich households. Fifth, the response of the risk premium to a TFP shock is highly state dependent and can even change sign depending on the distribution of wealth portfolios. These results underscore that the transmission of fiscal and monetary policy depends crucially on the cross-sectional distribution of households, with implications for the design and timing of stabilization policy.

The global solution framework is highly versatile and applies to a wide range of macroeconomic environments. The online supplement demonstrates this versatility through sample codes that address various computational challenges, including 1) heterogeneous agents—both households and firms; 2) nonlinear aggregate dynamics including occasionally-binding constraints; 3) non-trivial market clearing conditions; 4) multiple aggregate shocks (including aggregate uncertainty shocks (Bloom et al., 2018)); 5) multi-dimensional endogenous aggregate states; 6) frictional labor markets; and 7) sticky prices in New Keynesian models.[2]

---

[2]Ferreira et al. (2025) uses the RTM to solve a heterogeneous-firm general equilibrium model, studying the business cycle implications of corporate cash holdings. Also, Lee et al. (2024) applies the RTM to Diamond-Pissarides-Mortensen (DMP) models with exogenous and endogenous job separation to analyze nonlinear labor market dynamics. The RTM also solves nonlinear New Keynesian models globally and accurately.

Related literature The state space-based approach developed by Marcet (1988), Den Haan and Marcet (1990), and Krusell and Smith (1997, 1998), which uses parametric expectations or laws of motion, represents a foundational contribution to global solution methods.[3] While powerful for models with linear aggregate dynamics, this approach faces challenges with non-linear dynamics due to difficulties in correctly specifying the law of motion. These specification challenges can lead to inaccurate computation of conditional expectations and dynamic inconsistency in equilibrium paths. Den Haan and Rendahl (2010) advanced this literature by characterizing laws of motion through explicit aggregation of Taylor-approximated individual policy functions, enabling analysis of nonlinear dynamics. These methods share a common feature: they approximate conditional expectations through combinations of basis functions, which the repeated transition method (RTM) of this paper is sharply distinguished from.

Reiter (2010) is the closest to the RTM in its treatment of the endogenous state distributions in heterogeneous-agent models. The method introduces a reference distribution, characterized by a few moments, which is updated across iterations of the simulation. This reference distribution is then used to compute the conditional expectations of future (marginal) value functions without specifying a full law of motion. However, Reiter's approach remains anchored in the state space, as it categorizes aggregate distributions via their moments. As a result, it is still susceptible to the curse of dimensionality, particularly when higher-order moments or cross-sectional heterogeneity become salient. In contrast, the RTM translates this expectation-formation problem into the sequence space. By indexing value functions with time subscripts, RTM enables sharp identification of distributional states by matching across simulation periods — without requiring a moment-based summary or embedding distributions into the value function state space. This distinction allows the RTM to sidestep dimensionality issues: the model only needs to find a period where a similar distribution realized, not project distributions via a functional approximation. For the same reason, the RTM differs fundamentally from moment-based state approaches as in Den Haan (1996, 1997), Reiter (2001), Algan et al. (2008), and Algan et al. (2010) and functional approximations as in Cao et al. (2023) and Elenev et al. (2021).

While also operating in sequence space, the RTM differs fundamentally from Auclert et al.

Lee and Nomura (2024) applies the method to analyze the nonlinear inflation dynamics and Phillips curve outside and at the zero lower bound (ZLB). The method's ability to capture nonlinear dynamics enables analysis of state and history dependence that directly maps to empirical observations (Pizzinelli et al., 2020).

[3]The method of parameterized expectations traces back to Wright and Williams (1982, 1984) in the context of commodity storage models in partial equilibrium. Marcet (1988) and Den Haan and Marcet (1990) developed this approach for general equilibrium macroeconomic models, contributing methodological tools for modern heterogeneous-agent business cycle analysis.

(2021), which achieve remarkable computational efficiency through sequences of Jacobians. Their approach enables rapid likelihood-based estimation but requires perfect foresight. The RTM, in contrast, handles aggregate uncertainty while maintaining computational efficiency. This capability allows the method to accurately compute period-specific expected outcomes under uncertainty, distinguishing it from perfect-foresight approaches in the literature (Fair and Taylor, 1983; Juillard, 1996; Judd, 2002; Cai et al., 2017; Boppart et al., 2018). The RTM further differentiates itself by computing aggregate allocations and market-clearing prices directly on the simulated path without requiring law of motion specifications. This approach contrasts with perturbation and linearization methods (Reiter, 2009; Boppart et al., 2018; Ahn et al., 2018; Winberry, 2018; Childers, 2018; Bayer and Luetticke, 2020; Bhandari et al., 2023), providing a more direct route to equilibrium solutions.

The RTM shares important features with simulation-based methods developed by Judd et al. (2011) and Maliar et al. (2011), which achieve computational efficiency by focusing on the realized ergodic state space. The RTM builds on this insight while making a crucial advance: I use the information contained in the realized state space to construct agents' conditional expectations at each point on the simulated path, significantly improving solution accuracy.

My paper introduces the GTF, which nests generalized impulse response functions (GIRF) (Koop et al., 1996; Andreasen et al., 2017) and stochastic growth path (Justiniano and Primiceri, 2008; Hansen et al., 2008). As in Andreasen et al. (2017), the function can flexibly capture the nonlinearity and state dependence, but it computes the transition path based on global computation without high-order approximations. Unlike the existing GIRF, the GTF-based GIRF is a subpath of the recursive competitive equilibrium, which allows a unified analysis in comparison with the global equilibrium. The existing stochastic growth path has largely assumed a long-run stochastic growth by considering aggregate fluctuations on the balanced growth path. In contrast, GTF captures short-run stochastic growth path. The backward solution approach in the RTM and the time-dependent nonlinear dynamics in the GTF resembles the solution approach developed by Maliar et al. (2020). However, my paper's framework is about stationary but stochastic equilibrium dynamics process nested in the RCE, while their extended function path (EFP) approach is on non-stationary equilibrium dynamics utilizing turnpike property.

The findings from the leading applications contribute to the literature on nonlinear business cycle dynamics, particularly in studying state-dependent responses and the nonlinear propagation of aggregate shocks. A key prediction emerging from the RTM-GTF framework is the possibility of endogenous disaster-like downturns, conceptually related to the mechanism in Petrosky-Nadeau et al. (2018). However, while their model relies on frictions in the

labor market, the dynamics in my framework arise from the evolving cross-sectional distribution of marginal propensities to consume (MPCs) across households. The GTF analyses predict that the uncertainty dampens economic growth due to the down-sizing risk under the irreversibility constraint. This brings the wait-and-see prediction by Bloom et al. (2018) into the economic growth context in the stochastic environment. The model also predicts state-dependent fiscal multipliers, contributing to a growing body of work including Christiano et al. (2011), Kaplan and Violante (2014), Michaillat (2014), Shen and Yang (2018), Ghassibe and Zanetti (2022), and Jo and Zubairy (2025). In particular, the mechanism in my setting operates through labor supply elasticities that vary endogenously with the share of hand-to-mouth households—in line with the incomplete markets mechanism in Kaplan and Violante (2014). Importantly, however, my model departs from theirs by embedding this mechanism in a fully recursive competitive equilibrium (RCE) under aggregate uncertainty, which allows the distribution of constrained households to evolve endogenously. The application also sheds light on heterogeneous portfolio adjustments in response to business cycle fluctuations. In contrast to standard representative-agent or static-heterogeneity models, the RTM-GTF setup captures the dynamic reallocation between risky and riskless assets across households as the macroeconomic state evolves. This connects to the heterogeneous portfolio choice literature, including Den Haan (1996), Krusell and Smith (1997), Heaton and Lucas (2000), Gomes and Michaelides (2007), Basten et al. (2016), Fagereng et al. (2017), Fagereng et al. (2017), Bayer et al. (2019), Luetticke (2021) and more recently Auclert et al. (2024, 2025), which studies how heterogeneous portfolio choices interplay with the incomplete markets and aggregate risk. My model focuses on the interaction of borrowing constraints and labor income risk in the RCE and its state-dependent asset pricing implications.

Roadmap   Section 2 explains the repeated transition method. Section 3 explains the sufficient statistic approach. Section 4 explains how the RTM bypasses non-trivial market clearing conditions. Section 5 introduces the GTF. Section 6 analyzes the leading applications. Section 7 concludes.

2 The global nonlinear solution method in the sequence space

2.1 A generic model framework

This section introduces a generic model framework that encompasses a broad class of dynamic stochastic general equilibrium (DSGE) models. The framework's flexibility allows it

to accommodate both heterogeneous and representative agent specifications. I denote the individual state as x and the aggregate state as X. The individual state x is composed of the endogenous individual state a and the exogenous individual state s (the idiosyncratic shocks). The aggregate state X is composed of the endogenous aggregate states Φ and the exogenous aggregate state S (the aggregate shocks). The endogenous aggregate state Φ takes different forms depending on the model class. In heterogeneous agent models, it represents the distribution of individual states x, while in representative agent models, it captures the set of aggregate allocations.

$$\text{(Individual state)} \qquad x = \{a, s\} \tag{1}$$

$$\text{(Aggregate state)} \qquad X = \{\Phi, S\} \tag{2}$$

The idiosyncratic and aggregate shock processes are assumed to follow a Markov process with a transition matrix Π^s and Π^S, respectively. The value function is denoted as V. Following standard notation, variables with apostrophes indicate future period values. The objective function of an economic agent is composed of the contemporaneous part $f(y, x', x; X)$ and the expected future value. The agent maximizes the objective function by choosing (y, a'), where y is a vector of control variables that affects only the contemporaneous period. Then, the recursive formulation of an agent's problem is as follows:[4]

$$V(x; X) = \max_{y, a'} \ f(y, a', x; X) + \mathbb{E}m(X, X')V(a', s'; X') \tag{3}$$

$$\text{s.t.} \quad (y, x') \in \mathcal{B}(x; X, X', q), \quad \Phi' = F(X) \tag{4}$$

where $m(X, X')$ is the stochastic discount factor; $q(X, X')$ is a price bundle; $\mathcal{B}(x; X, X', q)$ is the budget constraint; $F(X)$ is the law of motion known to an individual agent.[5] For notational convenience, I combine the price bundle (m, q) into p. The following market clearing condition pins down the price p:[6]

$$[\text{Market clearing}]: \quad p(X, X') = \arg_{\widetilde{p}}\{Q^D(\widetilde{p}, X, X') - Q^S(\widetilde{p}, X, X') = 0\}, \tag{5}$$

---

[4]By expressing the model directly in recursive form, I implicitly assume the standard regularity conditions—namely, Assumptions 4.1 and 4.2 in Stokey et al. (1989).

[5]The stochastic discount factor can be a constant, for example β, as in a canonical dynamic household's problems. In a dynamic firm problem, the stochastic discount factor needs to be included.

[6]Any period-specific fixed point problem can be considered in the method, such as the externality effect as a function of endogenous allocations or non-trivial market clearing conditions. For brevity, I only include the non-trivial market clearing condition.

where Q^D and Q^S are the functions of demand and supply, which are endogenously determined by the model. The market clearing condition can be relaxed to a frictional price determination. For example, the method seamlessly works for the frictional labor market where the wage is bilaterally determined, as in Diamond-Pissarides-Mortensen (DMP) models, applications of which are available in the online supplements. For expositional clarity, I consider a simple case where the exogenous aggregate state S can take two possible values $\{G, B\}$ with a 2×2 transition matrix Π^S.[7] Based on this setup, Definition 1 defines the recursive competitive equilibrium (RCE).

Definition 1 (The recursive competitive equilibrium).
$(V, g_y, g_a) : \S \times \mathcal{X} \to \mathbb{R}$, $F : \mathcal{X} \to \Omega$, and $(Q^S, Q^D, p) : \mathcal{X} \times \mathcal{X} \to \mathbb{R}$ are the recursive competitive equilibrium if (i) (V, g_y, g_a) solves the agent's problem (ii) Q^D, Q^S represents the demands and supplies of inputs and outputs, (iii) p satisfies the market clearing condition, and (iv) F is consistent with the realized future distribution implied by g_a.[8]

In the following sections, I explain the method based on the recursive form in Equation (3) for the comprehensiveness of exposition. However, the method is seamlessly applied even if the value function is replaced by the first-order derivative or the marginal value functions. In the online supplement, I provide multiple applications where the expected marginal value function is computed instead of the expected value function.

My method achieves convergence in sequence space. Therefore, despite the converged equilibrium allocations being fully describable in a recursive form, I denote the equilibrium object in a sequential expression, such as $\{V_t\}$, for the sake of a coherent explanation. Hereafter, given a realized state $\{x_t, X_t\}$ for an individual (or representative) agent in a given period t, the value function in the sequential expression V_t and the value function in the recursive form $V(\cdot; X_t)$ are used interchangeably. The generic model framework nests the cases where the value function and the constraint allow the analytical expression of the first-order optimality conditions. In such cases, the marginal value function can replace the value function.

2.2 Assumptions

In this section, I discuss the key conditions a model must satisfy for the global solution method to be applicable. The method relies on three fundamental features: a) stability,

---

[7]The method's applicability is not limited to a certain number of grid points for the aggregate shocks. Moreover, multiple aggregate shocks can be considered an exogenous state.

[8]$\S, \mathcal{X}$ are the σ-algebras generated from all possible individual and aggregate states. Ω is a set of all distributions Φ.

b) uniqueness of the recursive competitive equilibrium (RCE), and c) recursivity of the equilibrium.

Recursivity, in particular, is essential: without it, certain equilibrium allocations may appear only once and never reoccur in the future, making it impossible to implement the method using repeated transitions. Specifically, I use "recursivity" to refer to Harris recurrence — the property that, regardless of the initial condition, the Markov process over state variables revisits equilibrium states with probability one.[9]

Combined with aperiodicity (i.e., the absence of deterministic cycles), these conditions guarantee the existence of a unique stationary distribution over the endogenous state variables — a distribution over distributions in heterogeneous-agent settings — from which ergodicity follows. In what follows, I focus exclusively on models that satisfy these three properties.

To ensure a well-defined equilibrium, I assume there is no redundancy in the representation of the aggregate state X. Specifically, I require a one-to-one mapping between the economy's fundamental state and the aggregate state X, formalized as:

$$V(x; X) = V(x; X') \text{ for } \forall x \quad \iff \quad X = X'. \tag{6}$$

This condition rules out redundant state variables that could artificially generate equilibrium multiplicity through superfluous expansions of the state space. Put differently, X is the natural minimal state variable (Cao, 2020).

2.3   The methodology

The method's key innovation lies in computing conditional expectations directly from realized equilibrium allocations of previous iterations. In particular, the method, which I name the *repeated transition method* (RTM, hereafter), exploits a fundamental property of DSGE models' recursive competitive equilibria - their *recursivity*. That is, if a simulated path of a stationary aggregate shock process is long enough, an endogenous aggregate state is almost surely revisited. Along with this recursion of the endogenous aggregate state, different exogenous aggregate states are stochastically realized on the path, forming an ergodic set of aggregate states. This ergodic set encompasses all the possible combinations

---

[9]The exact technical definition sharpens the statement by requiring that the Markov process revisit arbitrarily small neighborhoods of equilibrium states with probability one. Harris recurrence is implied under a set of standard regularity conditions: 1) the Feller property, 2) a Lyapunov drift condition (boundedness), 3) irreducibility, and 4) minorization. These are typically satisfied by dynamic macroeconomic models with smooth objective functions and bounded returns—see Assumption 4.2 in Stokey et al. (1989). For formal statements and proofs, see Chapter 4 of Stokey et al. (1989) and Chapter 9 of Meyn and Tweedie (1993).

of endogenous and exogenous aggregate states in equilibrium. This property implies that all state-contingent future allocations are obtainable as realized equilibrium outcomes somewhere on the sufficiently long simulated path.

Therefore, by identifying periods with equilibrium outcomes corresponding to each contingent future state from the previous iteration, the RTM characterizes an agent's conditional expectations at any point on the simulated path. The identifiability of such period is guaranteed by the *recursivity* (or by the *ergodicity*) of the RCE. Then, the conditional expectation converges to the true level (function) as iterations proceed, ensured by the *stability* and the *uniqueness* of the RCE. Notably, this approach eliminates the need to specify parametric laws of motion or expectations - the method requires only a metric to assess similarity between aggregate states across periods.

For a simple illustration, consider an agent's infinite-horizon dynamic problem under aggregate uncertainty with two possible exogenous aggregate states: G (Good) or B (Bad). To solve the agent's problem at period t, a researcher needs to construct the expected value (marginal value) function of period $t + 1$. The RTM accomplishes this by first identifying, for each possible future state $S_{t+1} \in \{G, B\}$, a period in the previous iteration's allocation path where the endogenous aggregate state most closely matches that of period t+1. The expected future value function is then constructed by combining the time-specific value functions from these identified periods. This approach works because the ergodicity of a sufficiently long simulation ensures the existence of periods where endogenous aggregate allocations (such as the distribution of individual states) match those of period t+1 under each possible shock realization. Consequently, the expected future value (marginal value) function at each period can be accurately constructed by combining these realized outcomes from the simulation path.[10]

The method iteratively updates the guessed (predicted) allocation path by using the realized allocation path in the past iteration until they converge to each other.[11] In these steps, each iteration passes over the information of the whole sequence of the realized allocations to the next iteration, utilizing the maximal set of information regarding the transition dynamics. This approach fundamentally differs from existing state-space methods, which restrict transition dynamics to functional relationships between current and future states. By avoiding such parametric specifications, the RTM accurately computes the equilibrium dynamics even in highly nonlinear models. Further, the required simulation length for the RTM is not longer than that for the existing methods, as the update based on the whole

---

[10]The method's name - repeated transition method - reflects its key feature of utilizing *repeated transitions* between the same (similar) endogenous states with different exogenous states.

[11]The terminology "predicted" means predicted from the perspective of researcher outside the model. It is equivalent to n^{th} guess for the allocation paths.

sequence utilizes all information about the dynamics, minimizing the information waste per marginal increase in the number of periods in a simulation.

The basic structure of the methodology is as follows: Suppose T periods of aggregate exogenous states $\{S_t\}_{t=0}^T$ are simulated, and hypothetically the simulated path is long enough to make almost all the possible equilibrium allocations happen on the path.[12] The solution process starts by conjecturing three time series: 1) value functions, $\{V_t^{(0)}\}_{t=0}^T$, 2) endogenous states $\{\Phi_t^{(0)}\}_{t=0}^T$, and 3) prices $\{p_t^{(0)}\}_{t=0}^T$. Using these guesses, I solve the allocations backward from the terminal period T to obtain the implied value function solution $\{V_t^*\}_{t=0}^T$, and simulate the economy forward using the solution. The forward simulation generates the time series of the endogenous states $\{\Phi_t^*\}_{t=0}^T$, and implied prices $\{p_t^*\}_{t=0}^T$ from the market-clearing conditions. Here the price p_t^* is the price implied by the market clearing condition, rather than the market clearing price. This distinction is discussed in detail in Section 4. The guess is then updated through convex combinations of prior guesses and realized allocations to form $\{V_t^{(1)}, \Phi_t^{(1)}, p_t^{(1)}\}_{t=0}^T$. While this broad approach shares similarities with perfect-foresight methods (Fair and Taylor, 1983), it differs fundamentally in the backward solution step due to its treatment of conditional expectations.

To clarify this point, consider period t in iteration $n + 1$, after solving backward from T to $t + 1$. Suppose the exogenous state at period $t + 1$ is G ($S_{t+1} = G$). To solve an agent's problem at t, one needs to construct an expected future value function $\mathbb{E}_t \widetilde{V}_{t+1}$.[13] This presents a challenge: while $V_{t+1}^*(\cdot, S = G)$ available from the backward solution, $V_{t+1}^*(\cdot, S = B)$ is not, as only one exogenous state realizes in each period. I define this unobserved $V_{t+1}^*(\cdot, S = B)$ as a *counterfactual* conditional value function.

The standard state space-based approach addresses this challenge by replacing time indices with endogenous and exogenous aggregate states, interpolating endogenous states through an assumed law of motion. The solution's accuracy thus critically depends on correctly specifying this law of motion. However, verifying the specification's accuracy is impossible before solving the equilibrium. An incorrect specification requires restarting the solution process with a new guess, presenting two fundamental challenges: determining which statistics to include and selecting appropriate functional forms. This problem cannot be easily resolved unless the aggregate dynamics are known to be log-linear, as in Krusell and Smith (1998).

---

[12] In theory, an infinitely long simulation needs to be considered, but for illustrative purposes, I consider a T-period long simulation. Later in the application, a long-enough finite simulation is used as an approximation for the infinitely long ergodic path. The RTM's reliance on a single, sufficiently long simulated path of aggregate shocks connects to recent work by Kahou et al. (2021).

[13] The method can potentially accommodate various expectation formations beyond rational expectations. The conditional expectation computation step can be adjusted to any well-defined expectation structure.

The RTM takes a fundamentally different approach. Instead of specifying a law of motion, it obtains the counterfactual conditional value function from another period $\widetilde{t}+1$ where the endogenous aggregate state matches that of period t+1 but realizes the counterfactual exogenous state:

$$\Phi^{(n)}_{\widetilde{t}+1} = \Phi^{(n)}_{t+1} \tag{7}$$

$$S_{\widetilde{t}+1} = B \neq G = S_{t+1}. \tag{8}$$

Under these conditions, all aggregate states in period $\widetilde{t}+1$ match those of the *counterfactual state* in period $t+1$, implying

$$V^{(n)}_{\widetilde{t}+1}(\cdot, S = B) = V^{(n)}_{t+1}(\cdot, S = B). \tag{9}$$

Importantly, $V^{(n)}_{\widetilde{t}+1}(\cdot, S = B)$ is the observed *factual* conditional value function available in the nth iteration. With both $V^{*}_{t+1}(\cdot, S = G)$ and $V^{(n)}_{t+1}(\cdot, S = B)(= V^{(n)}_{\widetilde{t}+1}(\cdot, S = B))$ available from iteration n, the expected future value function $\mathbb{E}_t \widetilde{V}_{t+1}$ can be consistently computed. This approach extends naturally to finer discretizations of the aggregate shock process.[14] The recursivity of the recursive competitive equilibrium ensures that such a period $\widetilde{t}+1$ exists almost surely in a sufficiently long simulation. Figure 1 illustrates the step for computing the conditional expectation in period t.
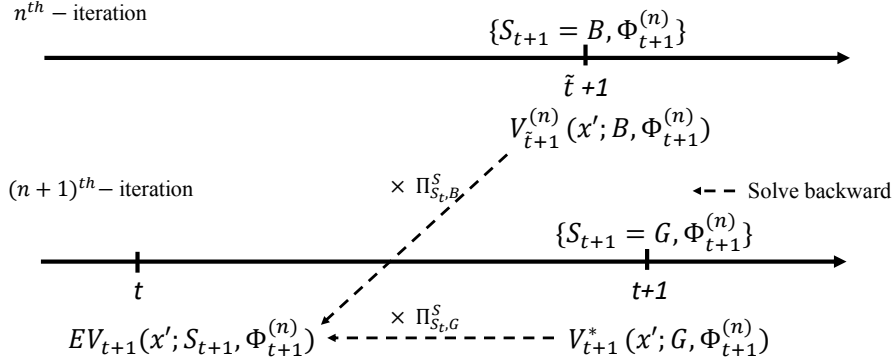
Figure 1: The computing step for conditional expectation based on the RTM

Notes: The conditional expectation in period t can be computed by $\mathbb{E}V_{t+1}(x'; S_{t+1}, \Phi^{(n)}_{t+1}) = \Pi^{S}_{S_t,B} \times V^{(n)}_{\widetilde{t}+1}(x'; B, \Phi^{(n)}_{t+1}) + \Pi^{S}_{S_t,G} \times V^{*}_{t+1}(x'; G, \Phi^{(n)}_{t+1})$.

This approach eliminates the need to specify a law of motion for computing expected future value functions. Instead, the critical step becomes identifying period $\widetilde{t}+1$ that

---

[14]Most applications in the online supplement employ finer grids than two grid points for the exogenous aggregate states.

replicates the counterfactual conditions of period $t+1$. This identification relies on tracking the sequence of endogenous aggregate states $\{\Phi_t^{(n)}\}_{t=0}^T$, which serves as the key criterion for locating appropriate matching periods:

$$\widetilde{t}+1 = \arg\min_{\tau} ||\Phi_\tau^{(n)} - \Phi_{t+1}^{(n)}|| \tag{10}$$

Taming curse of dimensionality The RTM efficiently tames the curse of dimensionality in two aspects. First, it replaces the infinite-dimensional law of motion by the uni-dimensional distance comparison. In the similarity comparison of the cross-sectional distributions, one needs to come up with a distance metric that is necessarily uni-dimensional.[15] This dimension reduction is independent of the sufficient statistic approach, which follows later. Second, the RTM indexes all the value and policy functions by time subscript, of which dimensions do not need to expand along the dimension of the aggregate state. In contrast, the state-space-based approach requires the dimensions of the value and policy functions to increase whenever the aggregate states expand.

The RTM algorithm

Step 1 (Initialization) Simulate a long path of aggregate shocks $\{S_t\}_{t=0}^T$. Conjecture initial sequences of value functions $\{V_t^{(0)}\}_{t=0}^T$, aggregate states $\{\Phi_t^{(0)}\}_{t=0}^T$, and prices $\{p_t^{(0)}\}_{t=0}^T$.

Step 2 (Backward solution) Starting from the terminal period T, solve agents' problems backward using expectations based on $\{V_t^{(n)}\}_{t=0}^T$. For each exogenous state in $t+1$:

   (a) Find periods τ such that $\Phi_\tau^{(n)} \approx \Phi_{t+1}^{(n)}$ and collect realized state-contingent value functions.

   (b) Use these values to construct expectations $E_t[V_{t+1}]$.

  Then, obtain the optimal value function V_t^* and the policy function g_t^{a*}.

Step 3 (Forward simulation) Simulate the model forward using $\{g_t^{a*}\}_{t=0}^T$ to generate $\{\Phi_t^*\}_{t=0}^T$ and implied prices $\{p_t^*\}_{t=0}^T$.

Step 4 (Update) Update the guessed sequences via convex combination:
$$V_t^{(n+1)} = \lambda V_t^* + (1-\lambda)V_t^{(n)}, \quad \text{similarly for } \Phi_t, \, p_t.$$

Step 5 (Iteration) Repeat Steps 2–4 until convergence:
$$\sup_t \left\| p_t^{(n+1)} - p_t^{(n)} \right\| < \varepsilon.$$

In the Online Appendix A, I elaborate on the detailed steps to implement the RTM and

---

[15]Otherwise, the closest distribution cannot be well-defined. If such a closest distribution does not exist, it violates the recursivity of the RCE.

the required length of the simulated path. Due to the method's ability to utilize the full information from the entire sequence, it requires no additional simulation length beyond what traditional methods demand. For example, as in Krusell and Smith (1998), if only two aggregate states are realized based on a symmetric transition probability of a moderate level (e.g., $\mathbb{P}(S' = G|S = B) = 0.125$), the simulation of less than 1,000 periods is enough to make the solution stay unaffected by further lengthening.[16]

3   A theory of sufficient statistic

While a large body of literature has employed sufficient statistics to address the curse of dimensionality in DSGE computation, the theoretical foundations justifying this approach have remained unclear. This section fills this gap by establishing precise conditions under which the sufficient statistic approach leads to an accurate solution. I first define the sufficient statistics.

Definition 2 (Sufficient statistics).
Consider a function $e : \Omega \to \mathbb{R}^n$. An equilibrium object $e_t := e(\Phi_t)$ is a sufficient statistic, if for $\mathcal{T}_S = \{t|S_t = S\}$, $\forall S \in \{B, G\}$,

$$e_t = e_{\widetilde{t}} \implies V_t = V_{\widetilde{t}}, \quad t, \widetilde{t} \in \mathcal{T}_S. \tag{11}$$

Notably, the sufficient statistic in the sequence space is differently defined from the counterpart in the state space. The latter finds $e_t = e(\Phi_t)$ as a variable that can literally replace or summarize Φ_t in the price determination or in the law of motion (Krusell and Smith, 1998; Alvarez et al., 2016; Baley and Blanco, 2021). In contrast, the sufficient statistic I define is an indexing variable where the same level of the variable indicates the periods with the same aggregate state. Therefore, the sufficient statistic does not necessarily replace or summarize the role of Φ_t in the sequence space. Instead, it provides proper indexation to help refer to the correct subset of time periods for forming the conditional expectation.

The assumptions in Section 2.2 establish a one-to-one relationship (bijection) between the sufficient statistic and the aggregate state. This result is formalized in Corollary 1 below.

Corollary 1 (Uniqueness and bijectivity).
If e_t is a sufficient statistic, given $S_t = S_{\widetilde{t}}$, the following relationship holds:

$$e_t = e_{\widetilde{t}} \iff \Phi_t = \Phi_{\widetilde{t}}. \tag{12}$$

---

[16]Appendix A.2 covers the required length of simulation path in detail.

Proof.

Due to the assumptions in Section 2.2, $e_t = e_{\widetilde{t}} \wedge S_t = S_{\widetilde{t}} \implies V_t = V_{\widetilde{t}} \implies \Phi_t = \Phi_{\widetilde{t}}$. From the definition of a sufficient statistic $\Phi_t = \Phi_{\widetilde{t}} \wedge S_t = S_{\widetilde{t}} \implies e_t = e(\Phi_t) = e(\Phi_{\widetilde{t}}) = e_{\widetilde{t}}$. ∎

The sufficient statistic is an $n-$dimensional vector. If such a sufficient statistic exists, the following set identity is obtained:

$$\arg\min_t ||e_t - e_{\widetilde{t}}|| = \arg\min_t ||\Phi_t - \Phi_{\widetilde{t}}||, \tag{13}$$

where the left-hand side problem is computationally lighter than the right-hand side due to the reduced dimension.

The RTM is particularly effective in handling multivariate sufficient statistics. Unlike traditional approaches, it does not require a parametric law of motion—an advantage when the relevant variables interact in high-dimensional or nonlinear ways. The only requirement is a similarity metric defined over the proposed sufficient statistic. Moreover, since the value and policy functions in the RTM are defined in the sequence space and indexed by time, their dimensionality does not increase when additional variables are included in the sufficient statistic. This allows the RTM to scale naturally to more complex state representations.

Extending this logic, even when the dimensionality of the sufficient statistic approaches that of the full aggregate state Φ_t, the dimensionality of the value and policy functions remains unchanged. This property enables a fully distributional implementation of the RTM, directly computing the right-hand side of Equation (13). Although this extension increases computational cost due to the pairwise high-dimensional distance computation, it remains a feasible and flexible option.

This computational flexibility enables a rigorous investigation on the existence of multiple self-fulfilling equilibria (Krusell and Smith, 2006; Cozzi, 2015). The literature has posited a conjecture regarding the existence of a self-fulfilling equilibrium due to the bounded-rational law of motion tracking the limited number of moments only. In the RTM, a heterogeneous-agent model can be solved by matching the entire distribution, which necessarily computes the recursive competitive equilibrium based on the full rational expectation. Then, two testings can be implemented: 1) a fitness of the bounded-rational law of motion can be tested based on this equilibrium path. Also, 2) the equilibrium path based on the bounded-rational law of motion can be directly compared to the equilibrium path with the full rationality under the same exogenous shock paths. I've implemented the second test for the model of Krusell and Smith (1998) and confirmed that the equilibrium paths between the bounded

15

rational law of motion and the full rationality are indistinguishably close to each other.[17]

Moreover, the RTM provides a useful proposition and practical test to enable a dramatic dimension reduction through the sufficient statistic as follows:

Proposition 1 (The monotonicity condition for a univariate sufficient statistic).
For each time partition $\mathcal{T}_S = \{t|S_t = S\}$, $S \in \{B,G\}$, if e_t is strictly monotone in V_t for $\forall t \in \mathcal{T}_S$ and all individual states (a,s), then, e_t is a sufficient statistic.

Proof.
Without loss of generality, assume $V_t < V_{\tilde{t}} \implies e_t < e_{\tilde{t}}$ for $\forall t, \tilde{t} \in \mathcal{T}_S$ and $\forall (a,s)$. From the contrapositive, $e_t \geq e_{\tilde{t}} \implies V_t \geq V_{\tilde{t}}$. Then, $e_t = e_{\tilde{t}} \iff e_t \geq e_{\tilde{t}} \wedge e_{\tilde{t}} \geq e_t \implies V_t \geq V_{\tilde{t}} \wedge V_{\tilde{t}} \geq V_t \implies V_t = V_{\tilde{t}}$. ∎

Proposition 1 establishes that when a time series $\{e_t\}_{t=0}^T$ *monotonically ranks* the level of the corresponding period's value function for each individual state, e_t qualifies as a sufficient statistic for period t in the RTM. The intuition behind the proposition is as follows. Consider a researcher searching for the appropriate value function to compute conditional expectations. If the correct counterfactual period τ were known explicitly, identifying the appropriate value function would be trivial since all value functions are indexed by time - V_τ would simply be the correct choice. Now instead of τ, suppose the level of e_τ is known to the researcher. Then, similar to the prior situation where τ is known, the researcher can identify which value function to use because the ranking information of e_τ uniquely pins down the corresponding value function due to the strict monotonicity. This monotonicity condition combined with Corollary 1 establishes a bijection between sufficient statistics and target periods, ensuring unique identification. The framework extends naturally to marginal value functions when solving models through first-order optimality conditions.

The monotonicity condition serves as a practically useful tester for the validity of a univariate sufficient statistic in the RTM. After the solution is obtained, I compute Spearman's rank coefficients between the sufficient statistic and the individual state-specific value functions for all individual states and for all aggregate exogenous states.[18] Next, I analyze the distribution of Spearman's rank correlation coefficients. In leading applications (and as in

---

[17]For the full rationality case, I use the following metric to measure the similarity of the distributions:

$$||\Phi_t - \Phi_{\tilde{t}}|| = \int (\Phi_t(x) - \Phi_{\tilde{t}}(X))^2 d\Phi_{\tilde{t}}(x). \tag{14}$$

In the computation, the updating weight for the $(n+1)^{th}$ guess needs to be set at a high level ($= 0.99$) for a smooth progression over iterations due to the possible nonlinear updates in the distributions (histogram).

[18]The Spearman's rank coefficient assess the monotonic functional relationship between two variables. The coefficient ranges from -1 to 1, and the two extreme levels of ± 1 imply the perfect monotonicity.

the online supplements), the sufficient statistic approach is validated as the average absolute Spearman coefficient remains close to unity.[19]

Remark 1 (Empirical test for a univariate sufficient statistic).
For each time partition $\mathcal{T}_S = \{t | S_t = S\}$, $S \in \{B, G\}$ and for all (a, s) if a univariate e_t satisfies

$$|Spearman(\{e_t\}_{t \in \mathcal{T}_S}, \{V_t(a, s)\})_{t \in \mathcal{T}_S}| = 1,$$

then, e_t is a sufficient statistic.[20]

Importantly, a sufficient statistic of the RTM may *not* qualify as a sufficient statistic in state space-based approaches. This is because the statistic does not necessarily include sufficient information about the inter-temporal dynamics of the endogenous aggregate state variables. As in Definition 2, the sufficient statistic in the RTM is an indexing variable for the cross-sectional similarity. For example, in the nonlinear model explained in Section 6, if I fit the nonlinear aggregate dynamics of the sufficient statistic obtained from the RTM to the nonlinear specifications of the single sufficient statistic, R^2 remains well below unity, indicating that one variable cannot adequately capture the full law of motion. Nevertheless, the variable alone serves perfectly as a sufficient statistic in the RTM by satisfying the monotonicity condition. This distinction highlights a key advantage of the RTM: it can achieve exact solutions with simpler sufficient statistics because it does not need to capture the full complexity of inter-temporal dynamics.

The first moment as the sufficient statistic   The first moment of the distribution, denoted by K_t, is one of the most natural and powerful candidates for a sufficient statistic. To formalize this idea, consider the following distance norm:

$$||\Phi_t - \Phi_{\tilde{t}}|| = \left| \int \omega(a, z) \mathcal{D}(\phi_t, \phi_{\tilde{t}}) d(a \times z) \right| \tag{15}$$

where ϕ_t is the probability density function (or histogram) associated with Φ_t. $\mathcal{D} : \mathbb{R}^2 \to \mathbb{R}$ denotes a difference metric. The function $\omega(a, z)$ is a weighting function that captures the relative importance of differences in the distribution. Suppose the weight is given by $\omega(a, z) = a$, reflecting the relative *economic* relevance of the individual state level in defining distance. Let the difference metric be the simple difference $d(x, y) = x - y$. Under these

---

[19]The monotonicity condition is a *sufficient* condition and *not* a necessary condition for a variable to qualify as a sufficient statistic. In other words, a variable e_t that does not monotonically rank V_t while satisfying conditions in Definition 2 could potentially exist.

[20]$Spearman(X, Y)$ denotes the Spearman's rank correlation coefficient between X and Y (Spearman, 1904).

choices, the distance norm simplifies to the absolute difference in the first moment:

$$||\Phi_t - \Phi_{\widetilde{t}}|| = \left| \int \omega(a,z)\mathcal{D}(\phi_t, \phi_{\widetilde{t}})d(a \times z) \right| \tag{16}$$

$$= \left| \int a\phi_t d(a \times z) - \int a\phi_{\widetilde{t}}d(a \times z) \right| \tag{17}$$

$$= |K_t - K_{\widetilde{t}}|. \tag{18}$$

This derivation offers a simple yet powerful insight into the role of the first moment: comparing first moments in sequence space can be interpreted as comparing distributions through economically weighted density differences. In the online supplement, more than ten models with rich micro-level heterogeneity are solved, and this approach proves to be highly effective, satisfying the monotonicity condition.

Moreover, $K_t = K_{\widetilde{t}}$ is a necessary for $\Phi_t = \Phi_{\widetilde{t}}$, making it a natural starting point for equilibrium computation. This is consistent with the standard strategy of solving for equilibrium using necessary conditions and verifying sufficiency via Proposition 1.

However, in some models, a univariate sufficient statistic may not exist. For example, consider an economy in which agents within a subgroup are homogeneous, but substantial variation exists across groups. In such cases, a vector of sufficient statistics is required to capture cross-sectional heterogeneity. Proposition 1 can be extended to these settings by introducing additional notation. Let $\mathcal{X}$ denote the set of all individual states $x = (a, s)$, and let $\{\mathcal{P}_j\}_{j=1}^n$ be a cross-sectional partition of $\mathcal{X}$ such that $\cup \mathcal{P}_j = \mathcal{X}$ and $\mathcal{P}_j$'s are pairwise disjoint.

Proposition 2 (The qualification for the multivariate sufficient statistic).
For each time partition $\mathcal{T}_S = \{t | S_t = S\}$ $S \in \{B, G\}$ and for cross-sectional partition $\mathcal{P}_j$, $j \in \{1, 2, \ldots, n\}$, if e_t^j is strictly monotone in V_t for $\forall t \in \mathcal{T}_S$ and $\forall (a, s) \in \mathcal{P}_t^j$, then, $e_t = (e_t^j)_{j=1}^n \in \mathbb{R}^n$ is a sufficient statistic.

Proof.
Without loss of generality, assume $V_t < V_{\widetilde{t}} \implies e_t^j < e_{\widetilde{t}}^j$ for $\forall t, \widetilde{t} \in \mathcal{T}_S$ and $\forall (a, s) \in \mathcal{P}_j$. From the contrapositive, $e_t^j \geq e_{\widetilde{t}}^j \implies V_t \geq V_{\widetilde{t}}$. Then, $e_t^j = e_{\widetilde{t}}^j \iff e_t \geq e_{\widetilde{t}} \wedge e_{\widetilde{t}} \geq e_t \implies V_t \geq V_{\widetilde{t}} \wedge V_{\widetilde{t}} \geq V_t \implies V_t = V_{\widetilde{t}}$. Therefore, $e_t = e_{\widetilde{t}} \implies e_t^j = e_{\widetilde{t}}^j$, for $\forall j \implies V_t = V_{\widetilde{t}}$ for $\forall t, \widetilde{t} \in \mathcal{T}_S$ and $\forall (a, s) \in \mathcal{X} = \cup \mathcal{P}_j$ ∎

In other cases, the failure of a univariate sufficient statistic arises from asymmetric non-linear effects of the distribution across individuals. When this occurs, the sufficient statistic must take the form of a vector of distributional moments—or, in the limiting case, the full distribution itself must be used within the RTM framework. Although the RTM is

well-suited to handling multivariate sufficient statistics, identifying counterfactual periods in high-dimensional space remains computationally demanding. Techniques from machine learning, such as clustering or deep learning, may offer practical solutions to reduce this burden.

4   Non-trivial market clearing conditions and accuracy

The RTM offers significant computational advantages, particularly in models with complex market clearing conditions. For instance, when applied to the Khan and Thomas (2008) model, the RTM converges nearly ten times faster than the Krusell and Smith (1997) algorithm.[21] This efficiency gain arises from a key methodological distinction: state-space-based approaches rely on computationally expensive nested loops to determine exact market-clearing prices each period, whereas the RTM utilizes implied prices that iteratively converge to equilibrium values. By eliminating the need for nested fixed-point calculations, the RTM achieves faster convergence without compromising accuracy. However, in cases where market clearing is straightforward—such as in the Krusell and Smith (1998) heterogeneous-agent model—the RTM's computational efficiency remains comparable to that of Maliar et al. (2010). The detailed comparison is available in Appendix C.

In the following, I elaborate on how the RTM efficiently handles non-trivial market clearing conditions and why this approach is infeasible in state space-based methods. Consider the following market clearing condition:

$$Q^D(p_t, X_t, X_{t+1}) - Q^S(p_t, X_t, X_{t+1}) = 0.$$
$$p_t := \arg_{\widetilde{p}}\{Q^D(\widetilde{p}, X_t, X_{t+1}) - Q^S(\widetilde{p}, X_t, X_{t+1}) = 0\}. \tag{19}$$

where Q^D and Q^S are demand and supply functions; p_t is the market clearing price; X_t and X_{t+1} are the current and future aggregate states. The market clearing condition is non-trivial when either demand, supply, or both lack closed-form characterization. For this problem, the RTM utilizes the implied price p_t^* instead of the exact clearing price p_t, where

$$p_t^* := \arg_{\widetilde{p}}\{Q^D(p_t^{(n)}, X_t, X_{t+1}) - Q^S(\widetilde{p}, X_t, X_{t+1}) = 0\} \text{ or}$$
$$:= \arg_{\widetilde{p}}\{Q^D(\widetilde{p}, X_t, X_{t+1}) - Q^S(p_t^{(n)}, X_t, X_{t+1}) = 0\}. \tag{20}$$

This approach fixes either demand or supply using the nth iteration's guessed price, then

---

[21]The RTM solves the model of Khan and Thomas (2008) in around 20 minutes, while the state-space-based approach takes longer than 7 hours. Computations use a MacBook Pro 2021 with M1 Pro chip.

finds the price that clears the remaining side. Computing this implied price is substantially simpler than finding the market clearing price, which requires solving a fixed-point problem where price simultaneously affects both supply and demand.

During the iteration, the implied price does not clear the market at each period, as it's only the implied price. However, as iteration goes by, the predicted path of prices $\{p_t^{(n)}\}_{t=0}^T$ converges to the equilibrium prices $\{p_t\}_{t=0}^T$. This convergence makes the implied price clear the market in the limit for the following reasons:[22]

$$\lim_{n \to \infty} Q^D(p_t^{(n)}, X_t, X_{t+1}) - Q^S(p_t^*, X_t, X_{t+1}) = 0 \tag{21}$$

$$\implies Q^D(\lim_{n \to \infty} p_t^{(n)}, X_t, X_{t+1}) - Q^S(p_t^*, X_t, X_{t+1}) = 0 \tag{22}$$

$$\implies Q^D(p_t, X_t, X_{t+1}) - Q^S(p_t^*, X_t, X_{t+1}) = 0 \tag{23}$$

$$\implies p_t^* = p_t \quad (\because \text{uniqueness of the equilibrium}). \tag{24}$$

Thus, the RTM's converged solution delivers exact market clearing prices alongside other equilibrium allocations.

In contrast, the implied price cannot replace the market clearing price in the state space-based approach (Krusell and Smith, 1997) in general. In their approach, the price dynamics is approximated by the parametric function of the aggregate state or the sufficient statistic, and the coefficients of the function carry the information about the relationship between the price and the aggregate state. Given that the number of coefficients cannot technically exceed the number of periods, the coefficients can only carry the summarized information. If the coefficients are updated based on the implied price rather than the market clearing price, the update is based on inaccurate levels, thus leading to a biased coefficient.[23] Then, the wrongly updated coefficients often lead to a divergent path, as there is no theoretical guarantee that the coefficient of the functional form features *stability*. The RTM, by contrast, preserves complete information about price-state relationships by carrying entire sequences through iterations. This approach enables uniform convergence in sequence space, guaranteed by equilibrium stability, without requiring functional approximations or coefficient estimation.

Computation accuracy　　I compare the repeated transition method with the other nonlinear solution methods in the literature for three DSGE models. The comparison is based on a real business cycle model with irreversible investment (McGrattan, 1996; Chris-

---

[22]The local continuity of demand or supply is necessary to proceed from the first to the second line. This should be true except for the knife-edge case where the unique equilibrium is at the discontinuity point, which DSGE models are barely subject to.

[23]While Bakota (2023) develops a method to update pricing rules approximately without exact market clearing, improving state space computation speed, the RTM bypasses the need for such approximations entirely.

tiano and Fisher, 2000), where I benchmark the RTM against three alternatives: linearized solution, the OccBin method of Guerrieri and Iacoviello (2015) and the GDSGE solution of Cao et al. (2023). The model features highly nonlinear aggregate dynamics due to the occasionally binding irreversibility constraint for capital investment. Therefore, besides the macroeconomic implications, the model serves as an ideal testing ground for the accuracy of the different methods for the nonlinear solutions. The RTM displays a higher accuracy than other methodology in terms of dynamic consistency and the Euler equation error.[24] Detailed comparisons is available in Appendix B. Notably, the RTM achieves its accuracy and speed using standard MATLAB code, without relying on lower-level machine languages or advanced econometric techniques.

5 Generalized Transition Function (GTF)

In this section, I define a generalized transition function (GTF), which is a sub-path of the recursive competitive equilibrium (RCE), and the RTM solution immediately computes the GTF. The GTF nests generalized impulse response functions (GIRF) (Koop et al., 1996; Andreasen et al., 2017) and stochastic growth path (Justiniano and Primiceri, 2008; Hansen et al., 2008).[25]

Definition 3 (Generalized transition function (GTF)).
Given an aggregate state realization (Φ_0, S_0) in the RCE, the generalized transition function g_j of the variable of interest v as follows:

$$g_j(v; \Phi_0, S_0) = \int v(x; \Phi_j, S_j)d\Phi_j, \quad S_j \sim \Gamma^j(S_j; S_0), \quad j \geq 1 \qquad (25)$$

where S_j is a random variable of the exogenous aggregate state, which follows a j-length Markov chain Γ^j from the initial realization of S_0.

Notably, Φ_0 is assumed to be a RCE allocation. However, a realistic analysis of the stochastic growth or structural transformation might need to consider Φ_0 off the RCE. Cao (2020) establishes the existence of dynamic stochastic competitive equilibrium (DSCE) paths starting from arbitrary initial points under mild assumptions that encompass variants of Krusell and Smith (1998). However, characterizing the initial DSCE path from a

---

[24]The RTM provides the realized allocation path implied by the prediction path (n^{th} guess). Dynamic consistency requires these predicted and realized paths to coincide. Thus, the RTM can serve as a diagnostic tool for other solution methods - by feeding their simulated paths as predicted paths into the RTM algorithm, it evaluates their dynamic consistency.

[25]The definition assumes an heterogeneous-agent setup with micro-level v for comprehensive explanation, but a representative-agent counterpart is consistently defined by omitting the integration.

non-equilibrium initial condition requires non-trivial computational steps due to its non-recursivity.[26] In computing the generalized transition function (GTF) from an initial state off the RCE, I assume that agents immediately adopt the policy function associated with the closest endogenous equilibrium state that shares the same exogenous state. This assumption is analogous to the saddle-path behavior in the canonical Ramsey growth model, where transversality conditions enforce an immediate jump to the stable manifold.

Definition 4 (An extended generalized transition function).
Given an aggregate state realization (Φ_0^{off}, S_0) off the RCE, the extended generalized transition function g_j of the variable of interest v as follows:

$$g_j(v; \Phi_0^{off}, S_0) = g_j(v; \Phi_0, S_0) = \int v(x; \Phi_j, S_j) d\Phi_j, \quad S_j \sim \Gamma^j(S_j; S_0), \quad j \geq 1 \qquad (26)$$

where $\Phi_0 = \arg \min_{\widetilde{\Phi} \in \Omega^{RCE}x} ||\Phi_0^{off} - \widetilde{\Phi}||$ and S_j is a random variable of the exogenous aggregate state, which follows a j-length Markov chain Γ^j from the initial realization of S_0.[27]

For brevity, I denote g_j as a transition function under the j'th exogenous state, so each g_j is also a random variable. Notably, $\mathcal{G} := \{g_1, g_2, \dots\}$ is a sub-path of the RCE. Therefore, $\mathcal{G}$ is readily computable from the global solution computed by the RTM. Specifically, for each (Φ_j, S_j), v can be obtained by identifying the period sharing the closest aggregate states in the global solution path and then interpolating the functions.

A certain magnitude of exogenous shocks is often considered in impulse response analyses. In the GTF, one can flexibly consider an arbitrary magnitude of the initial exogenous shock by fixing the initial exogenous state realization S_1. Still, this response path is a subpath of the RCE. I formally define the refined generalized impulse response function as follows:

Definition 5 (A refined generalized impulse response function).
Given an aggregate state realization (Φ_0, S_0) in the RCE, the refined generalized impulse response g_j^{girf} of the variable of interest v to an exogenous state realization S_1 in the following period is as follows:

$$g_1^{girf}(v; \Phi_0, S_0, S_1) = \int v(x; \Phi_1, S_1) d\Phi_1 \qquad (27)$$

$$g_j^{girf}(v; \Phi_0, S_0, S_1) = \int v(x; \Phi_j, S_j) d\Phi_j, \quad S_j \sim \Gamma^j(S_j; S_1), \quad j > 1 \qquad (28)$$

---

[26] If the state were recursive, it would already belong to the set of RCE allocations given the uniqueness of the RCE.

[27] Ω^{RCE} indicates all possible distributions in the RCE.

where S_j is a random variable of the exogenous aggregate state, which follows a j-length Markov chain from the initial realization of S_1.

Given Line (27), the first component of the g_1^{girf} is deterministic, as the magnitude of the shock $|S_1 - S_0|$ is set by a researcher from choosing S_1. The average path with the 95% confidence intervals can be characterized based on simulated shock paths.[28] Notably, the average GTF path is distinguished from the GTF path of average exogenous process due to the possible nonlinearity in the GTF. Also, the average GTF significantly deviates from the perfect-foresight growth path as studied in Section 6.1. The state dependence in the response path could be flexibly analyzed through varying Φ_0 and S_0 with $|S_1 - S_0|$ fixed.

6 Nonlinear heterogeneous-household business cycle models

The subsequent sections present two sets of analyses based on heterogeneous household business cycle models. These applications address important macroeconomic questions that have remained unexplored due to computational barriers. The RTM's methodological breakthrough enables efficient solutions to these challenging problems.

6.1 The leading application I: A heterogeneous-household model with endogenous labor supply, investment irreversibility, and fiscal spending shock

The first leading application is a heterogeneous-household business cycle model with endogenous labor supply, investment irreversibility, and both aggregate TFP and fiscal spending shocks. The model features a continuum of ex-ante identical households of unit measure in an infinite-horizon discrete-time economy.

The model environment is characterized as follows. Each household faces uninsurable idiosyncratic labor productivity shocks and makes endogenous labor supply decisions n. The temporal utility is assumed to be a log utility with a future discount factor $\beta > 0$. At the beginning of each period, households observe their individual states (wealth a and productivity z) and the aggregate state X, forming rational expectations about future aggregate conditions X'. Apostrophes denote next-period variables.

---

[28] As the global solution is already computed by the RTM that covers all the possible sub-paths of the RCE, computing the GTFs for a substantially large number of shock paths incurs almost zero extra computation cost.

The recursive formulation of a household's problem is as follows:

$$V(a, z; X) = \max_{c,n,a'} \; log(c) - \frac{\eta}{1 + \frac{1}{\chi}} n^{1+\frac{1}{\chi}} + \beta \mathbb{E} V(a', z'; X') \tag{29}$$

$$\text{s.t.} \quad c + a' = (1 + r(X))a + w(X)zn - T(X) \tag{30}$$

$$a' - (1 - \delta)a \geq \phi I^{ss} \tag{31}$$

$$\Phi' = \Gamma_X(X) \quad \text{(Aggregate law of motion)} \tag{32}$$

$$S' \sim \pi(S'|S), \quad z' \sim \pi(z'|z) \tag{33}$$

where V is the value function of a household; r and w are capital rent and wage that are determined at the competitive input factor markets. I_{ss} is the steady-state aggregate saving (investment) level. T is the lump-sum tax. χ is the Frisch elasticity parameter, and η is the labor disutility parameter. ϕ is the parameter that governs the degree of the saving irreversibility. Γ_X is the aggregate law of motion. The idiosyncratic productivity z follows a Markov process, where $\pi(z'|z)$ governs the transition probability.

I consider a production sector that operates using a CRS Cobb-Douglas production function:

$$\max_{K,L} \; AK^{\alpha}L^{1-\alpha} - w(X)L - (r(X) + \delta)K, \tag{34}$$

where A is the aggregate TFP, K and L are capital and labor input demands.

The aggregate state X includes following three components:

$$X = \{\Phi, A, G\}. \tag{35}$$

where Φ is the distribution of the individual states, A is TFP, and G is government demand. The first is endogenous aggregate state, and the others follow exogenous log AR(1) processes specified as follows:

$$log(A') = \rho_A log(A) + \sigma_A \epsilon \quad \epsilon \sim_{iid} N(0,1) \tag{36}$$

$$log(G') = (1 - \rho_G)log(\overline{G}) + \rho_G log(G) + \sigma_G \epsilon \quad \epsilon \sim_{iid} N(0,1) \tag{37}$$

where $\overline{G}$ is the steady-state government demand. For $j \in \{A, G\}$, ρ_j is the persistence parameter for the exogenous processes, and σ_j is the volatility parameter. These processes are discretized by the Tauchen method in the computation. I assume the simplest government setup where the budget is balanced by lump-sum tax collection: $T(X) = G$. By assuming this, the symmetric lump-sum tax is collected from heterogeneous households. For computation, I use the standard parameter levels in the literature, which are available in Appendix

D.

The recursive competitive equilibrium is defined based on the following market-clearing conditions:

$$\text{(Labor market)} \quad L(X) = \int zn(a, z; X)d\Phi \tag{38}$$

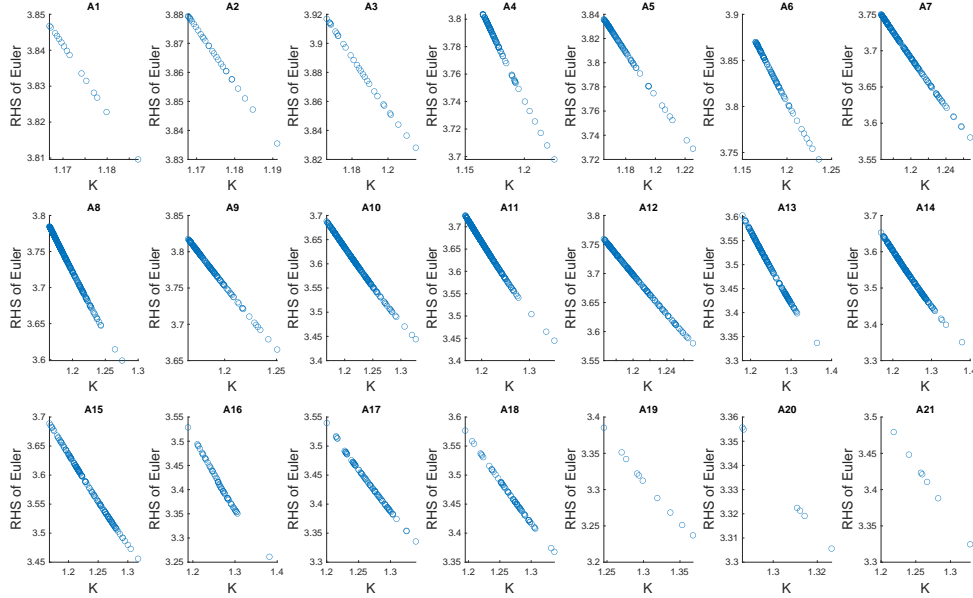$$\text{(Capital market)} \quad K(X) = \int ad\Phi. \tag{39}$$

Figure 2: Strict monotonicity of the marginal value in the aggregate capital stock

Notes: The figures are scatter plots of the marginal value functions in the vertical axis and the average capital as a sufficient statistic in the horizontal axis for different exogenous aggregate states (different panels) given the median level of individual wealth and productivity levels.

The market clearing is non-trivial as the wage determines individual labor supply, which needs to be aggregated instead of directly pinning down the aggregate labor supply. In Appendix D, I elaborate on how the RTM efficiently handles the model's non-trivial market clearing condition. Moreover, I verify the Proposition 1's monotonicity condition is sharply satisfied from the Spearman's coefficient test.[29] Figure 2 provides graphical evidence, plotting marginal values against aggregate capital stock across different TFP and government demand

---

[29]Specifically, I test the Spearman's coefficient between the sufficient statistic and the marginal value for each combination of individual states and exogenous aggregate states. The coefficient of unity implies the perfect monotonicity. In this analysis, the minimum coefficients among all combinations for both optimality conditions are distant from unity by 10^{-15}. The averages are not distinguishable from unity, and the standard deviations are around 10^{-16}. Thus, the monotonicity property holds robustly across the entire cross-section of the individual states.

levels ($7 \times 3 = 21$ exogenous states) with individual states fixed at median levels of wealth and labor productivity.

The solution reveals highly nonlinear dynamics in the aggregate capital path, driven by the occasionally binding constraint. Figure 5 compares three capital paths: the predicted path $\{K_t^{(n)}\}_{t=0}^T$, the realized (implied) path $\{K_t^*\}_{t=0}^T$ from the RTM, and a simulated path using a fitted log-linear law of motion. While the predicted and realized paths coincide to form the equilibrium solution, the log-linear approximation shows significant deviations.[30]
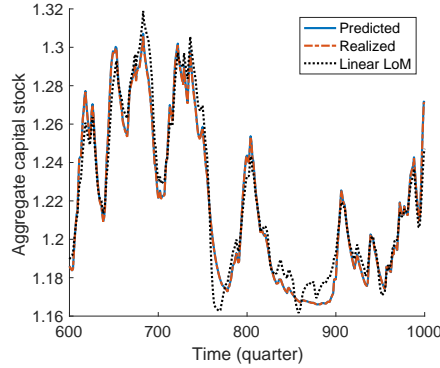

Figure 3: The equilibrium path of aggregate capital stock

Notes: The figure plots the time series of the aggregate capital stock K_t in the extended model of Krusell and Smith (1998). The solid line is the predicted capital (n^{th} guess) $\{K_t^{(n)}\}_{t=600}^{1000}$. The dashed line is the implied capital $\{K_t^*\}_{t=600}^{1000}$. The dotted line is the capital predicted by the linear law of motion.

6.1.1 Nonlinearity and aggregation

This section examines how micro-level nonlinearities shape aggregate dynamics by comparing heterogeneous and representative agent versions of the model. I contrast the heterogeneous-household model (HH) with a representative-household variant (RH) that eliminates labor productivity heterogeneity while maintaining all other parameter values. To ensure precise comparison, I apply identical aggregate TFP paths to both specifications and solve them using the RTM.

Figure 4 presents comparative dynamics in two contexts. Panel (a) displays equilibrium capital paths for the HH model (solid line) and RH model (dash-dotted line), expressed as log deviations from their respective steady states. For broader perspective, Panel (b) provides

---

[30]Fitting the aggregate capital dynamics to a log-linear $AR(1)$ specification with exogenous shock controls yields an R^2 of 0.920. As Den Haan (2010) demonstrates, such R^2 values can mask substantial inaccuracies in aggregate dynamics as shown in Figure 3. Achieving high accuracy requires considerably more complex specifications than log-linear forms (details available upon request).

an analogous comparison between heterogeneous-firm and representative-firm models subject to the same investment irreversibility constraint.[31]
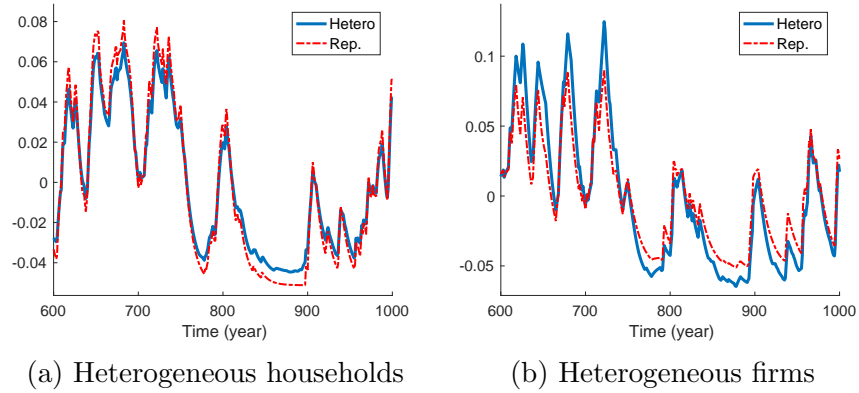

(a) Heterogeneous households   (b) Heterogeneous firms

Figure 4: Equilibrium dynamics comparison: Heterogeneous households vs. firms

Notes: Panel (a) plots the subsample of the equilibrium capital dynamics for heterogeneous household model (solid) and the representative household counterpart (solid). Panel (b) plots the subsample of the equilibrium capital dynamics for heterogeneous firm model (solid) and the representative firm counterpart (solid).

The analysis reveals striking differences in aggregate dynamics between heterogeneous and representative agent specifications. HH exhibits substantially lower capital stock volatility than RH, driven by reduced investment volatility. However, this volatility reduction does not stem merely from the presence of micro-level heterogeneity per se. Indeed, panel (b) demonstrates that heterogeneous-firm models display markedly higher capital stock volatility, stemming from increased investment volatility. This contrast highlights how the specific nature of heterogeneity shapes aggregate nonlinear dynamics.

The business cycle statistics reported in Table 1 quantify these differences. While the HH and RH models generate similar time-series averages, they differ notably in higher moments. The HH model produces lower volatility in both output (5% reduction) and investment (18% reduction), though consumption volatility remains similar between the specifications. The models also differ in asymmetry: the HH model exhibits more negative skewness in output and consumption, but more positive skewness in investment.[32]

Therefore, the representative-household model fails to adequately capture business cycle dynamics present in the heterogeneous-household model. The key driver of this misalignment is nonlinearity in household-level wealth dynamics.[33] To see this, I compute the same heterogeneous and representative household models without the occasionally binding irreversibility

---

[31]Online Appendix E provides detailed specifications for the heterogeneous-firm model with irreversible investment shown in Panel (b).

[32]Detailed business cycle statistics for the firm-side comparisons are provided in Appendix E.

[33]This result is specific to this model. For example, Khan and Thomas (2008) shows that the general equilibrium effect washes out the firm-level nonlinearity in their model.

Table 1: Business cycle statistics: heterogeneous (HH) vs. representative (RH)

	Heterogeneous	Representative
Mean		
Output	0.512	0.508
Consumption	0.288	0.287
Investment	0.122	0.120
Volatility		
$log(Output)$	0.042	0.044
$log(Consumption)$	0.057	0.058
$log(Investment)$	0.049	0.060
Skewness		
$log(Output)$	-0.026	0.024
$log(Consumption)$	-0.363	-0.349
$log(Investment)$	0.936	0.874

Notes: The table reports the business cycle statistics implied by the heterogeneous agent model (the first column) and the representative counterpart (the second column).

constraint (fully reversible investment), which is the source of the nonlinearity. Specifically, for the HH benchmark, the irreversibility constraint is replaced by zero borrowing limit constraint as in Krusell and Smith (1998) and Aiyagari (1994).
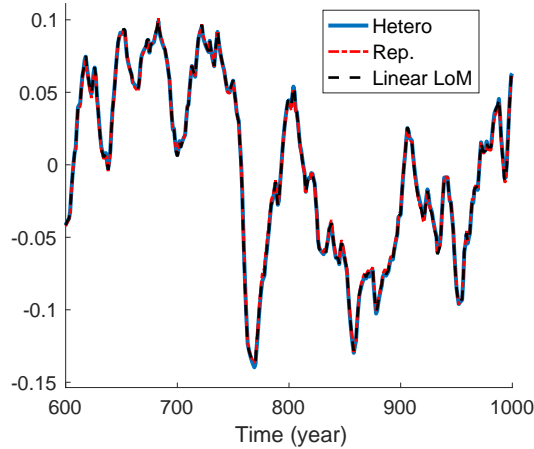

Figure 5: Equilibrium dynamics comparison - frictionless: Heterogeneous vs. representative

Notes: The figure plots the time series of the aggregate capital stock K_t in the extended model of Krusell and Smith (1998) without the irreversibility constraint. The solid line is the predicted capital (n^{th} guess) $\{K_t^{(n)}\}_{t=600}^{1000}$. The dashed line is the implied capital $\{K_t^*\}_{t=600}^{1000}$. The dotted line is the capital predicted by the linear law of motion.

Figure 5 plots equilibrium capital dynamics for these 'reversible benchmark' cases, showing log deviations from steady state alongside a fitted log-linear law of motion. The perfect alignment of all three paths demonstrates that when heterogeneous household decisions are (near-)linear, the representative agent model provides an almost exact characterization of

aggregate dynamics.[34]

6.1.2 State-dependent fiscal multipliers

State-dependent policy effects are a crucial feature of models with nonlinear aggregate fluctuations, yet analyzing these effects requires solution methods that can accurately capture global nonlinearities. The model in this paper provides an ideal laboratory for studying such state dependence through the lens of households' occasionally-binding constraints. The key mechanism operates through an asymmetric wealth adjustment constraint: households face greater friction when attempting to reduce their wealth positions than when increasing them. This asymmetry creates state-dependent marginal propensities to consume (MPCs), as households near their constraint exhibit nearly one-to-one consumption responses to negative income shocks while maintaining more modest responses to positive shocks.

The model's calibration generates patterns of household financial constraints that align remarkably well with empirical evidence. Using an irreversibility parameter of $\phi = 0.975$ used in Guerrieri and Iacoviello (2015), the model produces a steady-state share of 33.9% hand-to-mouth households, which is highly consistent with the empirical estimates from Kaplan and Violante (2014). Importantly, the model captures a key feature of household financial constraints: they affect not only low-wealth households but also wealthy ones who face temporary difficulties adjusting their wealth. This feature emerges naturally from specifying the constraint in terms of the wealth adjustment rather than the level of wealth. As a result, 21.6% of hand-to-mouth households in the model hold above-average wealth, consistent with the "wealthy hand-to-mouth" phenomenon documented in the literature.

A positive fiscal demand shock generates heterogeneous output responses that depend crucially on the distribution of financially constrained households. When a large fraction of households face binding constraints, the economy exhibits a powerful amplification mechanism: The lump-sum taxes levied to finance government spending trigger substantial declines in household consumption, which in turn induce a strong positive labor supply response through a wealth effect. This amplification mechanism leads to a significant increase in aggregate output, as illustrated in Equation (40). In contrast, when most households operate away from their constraints, the same fiscal shock induces a more muted response. These unconstrained households can smooth consumption through saving adjustments, resulting in a smaller labor supply response and consequently a more modest output expansion, as

---

[34]The hand-to-mouth households in Krusell and Smith (1998) and Aiyagari (1994) display kinked saving policy around the borrowing limit. However, their contribution to the aggregate capital dynamics is almost negligible.

shown in Equation (41).

$$[Mostly\ constrained]: \quad \underbrace{C_t}_{\downarrow\downarrow\downarrow} + \underbrace{I_t}_{\downarrow} + \underbrace{G_t}_{\uparrow\uparrow} = Y_t \ \Uparrow \quad (\because \text{Large wealth effect}) \qquad (40)$$

$$[Mostly\ unconstrained]: \quad \underbrace{C_t}_{\downarrow\downarrow} + \underbrace{I_t}_{\downarrow\downarrow} + \underbrace{G_t}_{\uparrow\uparrow} = Y_t \ \uparrow \quad (\because \text{Small wealth effect}) \qquad (41)$$

To quantify this state dependence empirically, I estimate the following regression using simulated data from the model's global solution:

$$Y_t = \beta_0 + \beta_1 G_t + \beta_2 G_t \times \Lambda_t + \beta_3 log(K_t) + \beta_3 log(A_t) + \epsilon_t, \qquad (42)$$

where Y_t is aggregate output; G_t is government demand measured in the unit of output; Λ_t is the aggregated Lagrange multiplier defined by $\Lambda_t = \Lambda(X_t) := \int \lambda(a, z; X_t) d\Phi_t$. Λ_t captures both the portion of constrained households and the average binding intensity. The coefficient of primary interest is β_2, which captures how the fiscal multiplier varies with the prevalence of binding constraints.

The baseline HH specification without interaction terms yields a fiscal multiplier of approximately 0.8 over a two-year horizon, aligning with empirical estimates from Ramey (2020). However, incorporating state dependence through the interaction term reveals that this average effect masks substantial variation: the direct effect β_1 becomes notably smaller, while the interaction term accounts for roughly 23.5% of output variation ($= std(\widehat{\beta}_2 G_t A_t)/std(Y) \approx 23.5\%$). The model achieves remarkable fit after including state dependence, with mean squared prediction errors below 10^{-6}.

The result indicates that the fiscal multiplier is greater when a greater portion of households are constrained, which endogenously fluctuate over the business cycle. Importantly, this implies strong counter-cyclical variation in fiscal policy effectiveness in equilibrium: the negative correlation (-0.788) between output Y_t and the constraint intensity measure Λ_t indicates that borrowing constraints bind more frequently during economic downturns. This pattern implies that fiscal stimulus becomes particularly potent precisely when the economy is weak, providing a natural stabilization mechanism through state-dependent multipliers.

The third column presents the regression coefficients when the data is simulated from the RH model. Notably, the degree of state dependence in HH remains largely unchanged in its representative-agent counterpart. The fourth column reports the coefficients under the GHH utility specification, which eliminates the wealth effect arising from tax-driven consumption reductions. When using contemporaneous consumption C_t as the dependent variable in the same regression setup with the GHH utility, the results confirm that a fiscal demand shock significantly reduces consumption, consistent with both the HH and RH models. However,

Table 2: State-dependent fiscal spending multipliers

	Dependent variable: Y_t (\$)			
	Hetero. (HH)		Rep. (RH)	GHH
G_t (\$)	0.402	0.182	0.206	0.000
	(0.005)	(0.002)	(0.000)	(0.001)
G_t (\$) $\times \Lambda_t$		0.533	0.534	0.000
		(0.003)	(0.002)	(0.000)
$log(K_t)$	0.143	0.105	0.104	0.496
	(0.002)	(0.001)	(0.000)	(0.000)
$log(A_t)$	0.463	0.598	0.591	1.504
	(0.001)	(0.001)	(0.001)	(0.000)
Constant	Yes	Yes	Yes	Yes
Observations	3,000	3,000	3,000	3,000
R^2	0.992	0.999	0.999	0.999
Adjusted R^2	0.992	0.999	0.999	0.999

Notes: The table reports the regression results based on specification (42). The first two columns are results based on the heterogeneous household baseline model. The next column is based on the representative-household counterpart. The last column is based on the representative household model with GHH utility, where the wealth effect is muted.

this does not translate into any effect on aggregate output, as indicated by the near-zero estimates for β_1 and β_2. These findings highlight that the state-dependent fiscal multiplier operates through variations in the state-dependent MPC and the resulting wealth effect. In this context, the key equilibrium property of interest is global nonlinearity, which the RTM effectively captures by providing an accurate solution in sequence space.

6.1.3 The GTFs: an endogenous disaster and the stochastic growth path

Due to the model's nonlinear nature, the responsiveness of aggregate variables to an exogenous shock depends critically on the prevailing aggregate state. In particular, the size of the hand-to-mouth population plays a key role: identical shock paths can produce markedly different outcomes depending on its share. To analyze this state dependence, I use the generalized impulse response function (GIRF) constructed through the generalized transition function (GTF).

I identify two periods within the sequence of global equilibrium allocations in which the exogenous states are identical at their median levels, but the share of hand-to-mouth households differs substantially: The high hand-to-mouth share is approximately 43.7%, and the low share is approximately 34%. Figure 6 illustrates the responses of aggregate output (panel (a)) and aggregate consumption (panel (b)) to a negative two-standard-deviation TFP shock. The solid line corresponds to a state in which a large share of households are
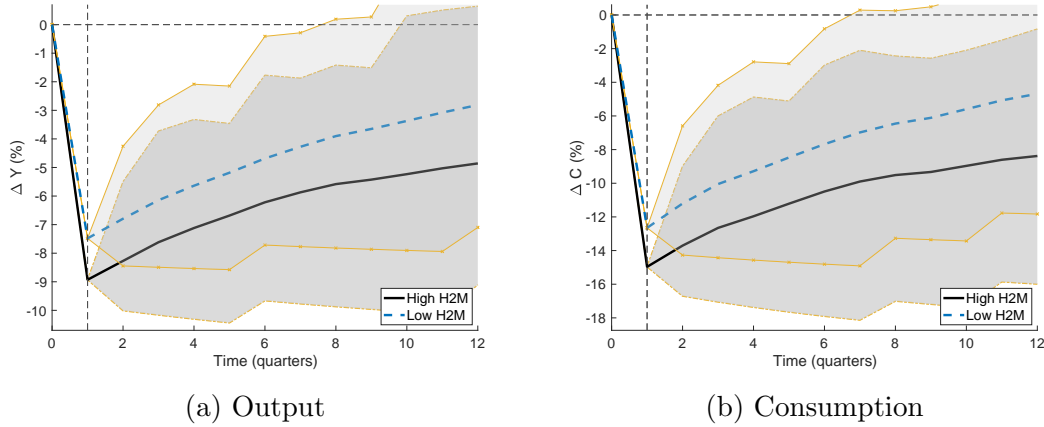
(a) Output   (b) Consumption

Figure 6: State-dependent responsiveness: high vs low hand-to-mouth portion

Notes: Panel (a) plots the generalized impulse response functions (GIRF) of output when the aggregate states before the shock hits were with a high portion hand-to-mouth households (solid line) and with a low portion of hand-to-mouth households (dashed line). Panel (b) plots the GIRFs of consumption. The shaded areas indicate the 95% confidence interval.

hand-to-mouth, while the dashed line reflects a state with a smaller hand-to-mouth share.[35]

Although the two states experience identical exogenous shock paths, their macroeconomic responses differ significantly. In the high hand-to-mouth state, output declines by around 28% more and aggregate consumption falls by 25% more compared to the low hand-to-mouth case. The key amplifying channel in the propagation of TFP shock is excess consumption shock sensitivity stemming from the high level of the cross-sectional average MPC. The consumption wealth effect channel does not effectively save the economy from the recession when there are large portion of hand-to-mouth people. It is because the constrained households are mostly with low labor productivity, so their increased labor supply motivated by wealth effect only marginally improve the aggregate labor supply. This state-dependent nonlinearity resonates with the concept of an *endogenous disaster* as studied in Petrosky-Nadeau et al. (2018). This result highlights that the macro economy's response to shocks depends not just on the size of the shock, but on the distributional state of the economy at the time the shock hits—a distinctively nonlinear feature enabled by the global solution method.

The generalized transition function (GTF) also provides valuable insights into stochastic growth dynamics. I examine a transition scenario beginning from an initial steady state with TFP 5% below the calibrated baseline. From this starting point, the economy evolves along stochastically determined growth paths reflecting various possible shock realizations. Figure 7 contrasts the stochastic growth path (solid line) of aggregate capital with the perfect-foresight growth path (dashed line). The comparison reveals two key findings: the

---

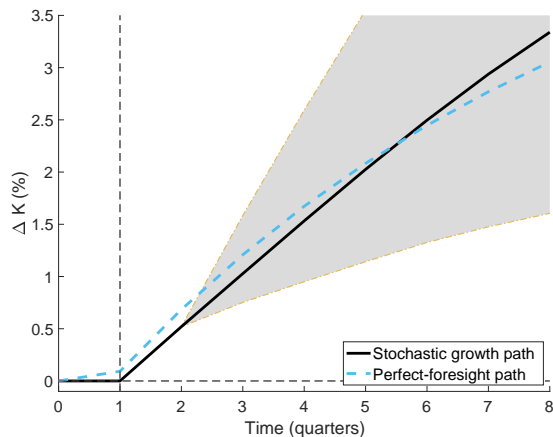[35]Both initial states share the same exogenous conditions: $A = 1$ and $G = 0.1011$.

Figure 7: Stochastic growth path vs. perfect-foresight growth path

Notes: The figure plots the GTF-based stochastic growth path (solid line) in comparison with the perfect-foresight growth path (dashed line). The shaded areas indicate the 95% confidence interval. The transition is initiated from the steady state of an economy with a 5% lower aggregate TFP productivity.

stochastic path exhibits slower initial growth on average, yet ultimately converges to a higher capital level than its perfect-foresight counterpart.

This divergence stems from fundamental differences in the households' expectations. The perfect-foresight path shows accelerated early growth precisely because households face no risk of having to downsize capital. In the stochastic environment, however, households must account for potential binding irreversibility constraints, leading to more cautious initial capital accumulation. According to the model, the uncertainty lowers the capital growth rate by up to 13 percent per quarter compared to the perfect foresight path.

Aggregate uncertainty ultimately drives greater capital accumulation through heightened precautionary saving motives, as evidenced by the higher long-run capital level in the latter phase of the transition. Together, these results highlight a novel interaction between growth dynamics and aggregate uncertainty—an underexplored but economically significant feature of dynamic stochastic economies.

6.2 The leading application II: A heterogeneous-household model with portfolio choice and endogenous labor supply

In this section, I analyze a heterogeneous-household business cycle model with portfolio choice, where each household endogenously determine labor supply. A continuum of unit measure of households who consumes, saves in two assets (capital and bond), and supplies

33

labor, which is summarized by following recursive formulation:

$$V(a,b,z;X) = \max_{c,n,a',b'} \frac{c^{1-\sigma}}{1-\sigma} - \frac{\eta}{1+\frac{1}{\chi}} n^{1+\frac{1}{\chi}} + \beta \mathbb{E} V(a',b',z';X') \tag{43}$$

$$\text{s.t. } c + a' + q^b(X)b' = a(1+r(X)) + b + zw(X)n \tag{44}$$

$$a' \geq 0, \quad b' \geq \underline{b} \tag{45}$$

$$\Phi' = \Gamma_X(X) \quad \text{(Aggregate law of motion)} \tag{46}$$

$$S' \sim \pi(S'|S), \quad z' \sim \pi(z'|z) \tag{47}$$

where c is consumption; z is idiosyncratic labor productivity, which follows a log AR(1) process; n is endogenously chosen labor supply; w is wage to be competitively determined at the factor input market, which thereby indicates that $zw(X)n$ is the labor income; a is the risky asset (capital) that earns capital rent $r = r(X)$ in each period, which is competitively determined at the capital market; b is the risk-free bond holding of which the price is $q = q(X)$. The bond price is competitively determined at the bond market. Apostrophe indicates future allocation. σ is risk-aversion parameter; χ is the Frisch labor elasticity; η is the labor disutility parameter; β is the discount factor. $\underline{b} \leq 0$ is the borrowing limit for future bond holding, and future risky asset is bound by zero borrowing limit.

The aggregate state X is defined as follows:

$$X := \{\Phi, A\} \tag{48}$$

where Φ is the joint distribution of the individual states; A is aggregate productivity that follows the same two-state Markov chain as in Krusell and Smith (1997). The rest of the model ingredients are identical to the leading application I (Section 6.1) except for the following bond market clearing condition: The bond price $q^b(X)$ is determined at the competitive market as follows:

$$[q]: \quad \int b'(\omega, z; X) d\Phi(X) = 0 \tag{49}$$

where I assume the aggregate net bond supply is zero as in Krusell and Smith (1997). I use the standard parameter levels in the literature, which are available in Appendix C.

The model includes two inter-temporal assets, which necessarily leads to a highly complex endogenous aggregate state in equilibrium. Moreover, the model includes two occasionally binding constraints and the two non-trivial market clearing conditions for labor and bond market, which exponentially increases the computational burdens. Nevertheless, the RTM efficiently computes the global solution. I elaborate on the computational details in Appendix E.

The bond market presents a unique computational challenge beyond standard market clearing issues: zero net supply $(B'(X) = 0)$ creates difficulties in characterizing the implied bond price using the RTM. The clearing condition reduces to a non-invertible identity: $q^b(X) \times B'(X) = B \iff q^b(X) \times 0 = 0$. This challenge becomes apparent when examining the national accounting identity derived from aggregating individual budget constraints:

$$C(X) + K'(X) + q^b(X)B'(X) = K(1 + r(X)) + B + w(X)N \tag{50}$$

$$\iff C(X) + I(X) + q^b(X)B' - B = Y(X) \tag{51}$$

$$\implies q^b(X)B' = B \iff q^b(X) \times 0 = 0, \tag{52}$$

where (C, K, I, Y, B) are aggregate consumption, capital stock, investment, output, and bond holdings. To overcome this computational challenge, I introduce a dummy bond term $\overline{B} > 0$, which remains fixed over the iterations. The dummy bond serves as a reference point for relative price updates. Specifically, this allows characterization of the implied price q^{b*} through

$$q_t^{b*}\overline{B} := Y_t^{(n)} - C_t^* - I_t^* + B_t^* + q_t^{b(n)}\overline{B} \implies q_t^{b*} = \frac{Y_t^{(n)} - C_t^* - I_t^* - B_t^* + q_t^{b(n)}\overline{B}}{\overline{B}}, \tag{53}$$

where asterisks denote aggregations of individual optimal choices given the nth iteration's guessed price path.[36] Through iteration, this approach achieves two convergence results: the implied bond price sequence $\{q_t^{b*}\}_{t=0}^T$ converges to market-clearing levels, and the aggregate net bond supply $B_t^* = \int b_t^* d\Phi$ converges to 0 for $\forall\, t$.[37]

6.2.1 Nonlinear bond price and heterogeneous portfolio adjustment over the business cycle

The RTM computes the equilibrium paths of the price bundle $(r(X), w(X), q(X))$. Among the prices, the bond price dynamics is particularly nonlinear, as can be seen from Figure 8. The predicted path (solid line) and the realized path (dash-dotted line) are indistinguishably close, which demonstrates the solution's accuracy. Its dynamics significantly deviate from the log-linear prediction (dotted line) based on the sufficient statistic $K(X)$. The fitted line's R^2 is only around 0.50, underscoring the inadequacy of linear approximations.

This finding has important implications for solution methods. The bond price's true law of motion is too complex for conventional state-space approaches, which would re-

---

[36]Appendix F explains the details of the role of the dummy bond variable.

[37]The equilibrium path shows high sensitivity to bond price adjustments, necessitating conservative updating (weight = 0.999) in the implementation. An alternative specification for the implied bond price is $q_t^{b*} = \frac{B_{t+1}^{(n)} - q_t^{b(n)}\overline{B}}{\overline{B}}$, which also leads to the convergent outcomes.

quire correctly specifying the functional form before solving the model. Yet notably, despite this complexity in price dynamics, the inter-temporal optimality conditions maintain strict monotonicity in the sufficient statistic K, as demonstrated by the Spearman's coefficient indistinguishably close to unity.[38] This result demonstrates a key advantage of the RTM: its sufficient statistic approach remains valid even when linear prediction rules fail, enabling accurate solutions to models with complex nonlinear dynamics without requiring explicit functional forms. The heterogeneous agent model generates bond price dynamics that
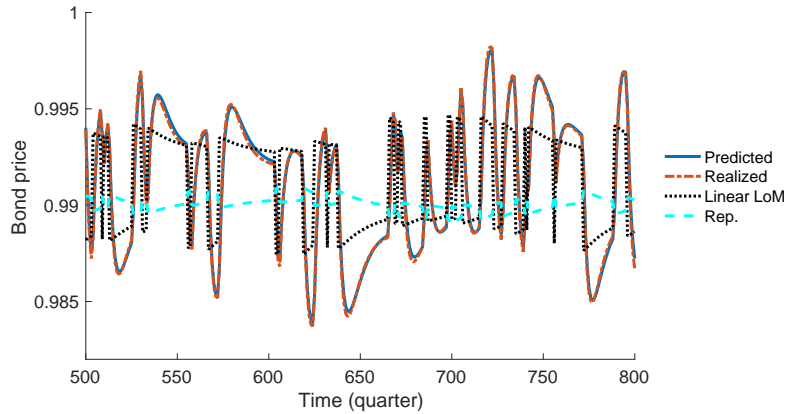

Figure 8: The equilibrium bond price path

Notes: The figure plots the time series of the bond price q_t^b in the extended model of Krusell and Smith (1997). The solid line is the predicted bond price (n^{th} guess) $\{q_t^{b(n)}\}_{t=500}^{800}$. The dashed line is the implied bond price $\{q_t^{b*}\}_{t=500}^{800}$. The dotted line is the bond price predicted by the linear law of motion.

sharply contrast with representative agent predictions.[39] The difference manifests in both cyclicality and volatility. While the heterogeneous agent model predicts pro-cyclical bond prices ($corr(Y_t, q_t^b) = 0.64$), while the representative agent framework implies counter-cyclical prices ($corr(Y_t, q_t^b) = -0.43$). The volatility difference is also striking: the heterogeneous agent model produces bond price volatility more than 9 times greater than its representative agent counterpart. These substantial differences stem from the rich heterogeneity in households' hedging motives across individual states, an equilibrium feature that representative agent models necessarily abstract from.

The global nonlinear solution of the model reveals a novel prediction about heterogeneous portfolio adjustment *over the business cycle* across different households. Due to the rich heterogeneity in the equilibrium in the dimensions of wealth, income, productivity, and

---

[38]The details of the test is availabe in Appendix D.

[39]In the representative agent model, the bond price is derived from the inverse of the risk-free rate. This remains an implied price since the zero net bond supply precludes actual transaction by the representative agent.

portfolio composition, the model provides various testable implications from the data. In the following analysis, I focus on the different portfolio adjustment patterns through the lens of the wealth heterogeneity. The analyses based on the labor income (productivity) heterogeneity are provided in Appendix G, which show consistent patterns as the one about the wealth heterogeneity.

Figure 9 illustrates this heterogeneity by tracking the household-level average of the risky asset weight in the portfolio for three groups: wealth-rich households (defined as those in the top tercile of the wealth distribution), wealth-poor households (those in the bottom tercile), and middle class (the remaining middle 40%), plotted against output deviations from steady state.

The wealth-rich and middle-class households display a highly stable individual portfolio weight over the business cycle, while the wealth-poor households dramatically rebalance their portfolios: the wealth-poor households display markedly counter-cyclical portfolio adjustments, increasing their risky asset allocations with a one-period lag relative to output fluctuations. First, this shows that less constrained households behave as if there is the optimal portfolio weight that does not vary over the business cycle. The middle-class households portfolio weight is stably (mildly fluctuating) formed at around 110% which implies they maintain risky asset weight by leveraging in the debt market. The constrained households' (wealth-poor) portfolio weight dramatically fluctuate around 100%, which indicates that they borrow and pay back debts flexibly over the business cycle.
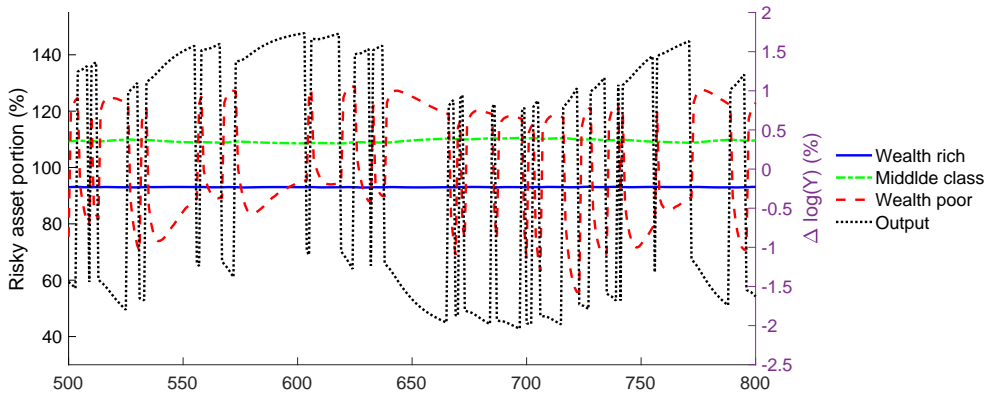

Figure 9: The time series of average risky asset portion across different wealth groups

Notes: The figure plots the time series of the risky asset portion (%) in the wealth portfolio for different households in the extended model of Krusell and Smith (1997). The solid line represents households in the top wealth tercile, while the dashed and the dash-dotted lines show households in the bottom wealth tercile and the remaining middle class. The dotted line depicts output (measured as percentage deviation from steady state), with values shown on the secondary vertical axis at the right side of the figure.

Figure 10 contrasts the asset holdings of different wealth groups in the consumption goods

unit (dollar) against output deviations from steady state, with panel (a) showing risky asset holdings and panel (b) displaying risk-free asset positions. Panel (a) demonstrates that richer households maintain larger risky asset positions, consistent with the empirical observation by Calvet et al. (2009). Panel (b) reveals the financing strategy behind these positions: wealth-poor and middle-class households achieve their risky asset holdings through leverage. Especially, wealth-poor households aggressively relies on borrowing to purchase risky assets, maintaining risk-free borrowing positions consistently near the constraint ($\underline{b} = -2.4$). In contrast, wealth-rich households hold large and stable risk-free asset positions throughout the business cycle.

A notable pattern observed from Figures 10 and 9 is that the wealth-poor households' average individual level portfolio weight dramatically fluctuate over the business cycle, while the group-level average does not fluctuates. This is because the risk-free asset and risky-asset transactions are the most active within the group of the wealth-poor households. From the policy perspective, these results imply that government's debt financing by issuance of risk-free bonds would lead to a significantly asymmetric impact on different wealth groups: the wealth-poor would face the most dramatic impact due to their highly volatile transactions of the bonds, which sharply deviates from the policy impact of the lump-sum tax financing. Also, the stark differences in the individual average and the group-level average show that the idiosyncratic shocks affect the heterogeneous decisions for the households close to the constraint.

These patterns offer important insights for both inequality dynamics and asset pricing theory. The global solution framework reveals how the bond market mediates heterogeneous hedging motives across household types, generating highly nonlinear and volatile bond prices. This interaction between household heterogeneity and financial markets provides novel perspectives on both inequality transmission and asset pricing mechanisms.

6.2.2 State-dependent GTFs of the risk premium

The model predicts highly nonlinear risk premium dynamics. Figure 11 illustrates the state-dependent impulse responses of the risk premium following TFP shocks of $\pm 2\%$, using the generalized transition function (GTF). Panel (a) shows the response to a negative TFP shock, while panel (b) shows the response to a positive TFP shock. The key state variable that differentiates the responses is the portfolio composition prior to the shock—specifically, the economy's aggregate exposure to the risky asset.

In response to a negative TFP shock (panel (a)), the risk premium declines sharply in economies that enter the shock with low risky asset holdings (dashed blue line). This reflects low expected risky return followed by flexible portfolio adjustments in a relatively less
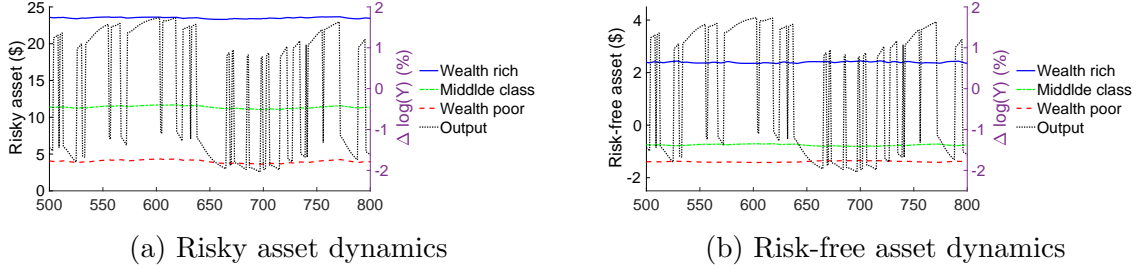
38

(a) Risky asset dynamics   (b) Risk-free asset dynamics

Figure 10: Risky and risk-free asset holding dynamics across different wealth groups

Notes: The figure plots the time series of the different asset holdings ($) by household types in the extended model of Krusell and Smith (1997). Panel (a) is for the risky asset, and panel (b) is for the risk-free asset. The solid line represents households in the top productivity tercile, while the dashed line shows households in the bottom productivity tercile. The dotted line depicts output (measured as percentage deviation from steady state), with values shown on the secondary vertical axis at the right side of the figure.
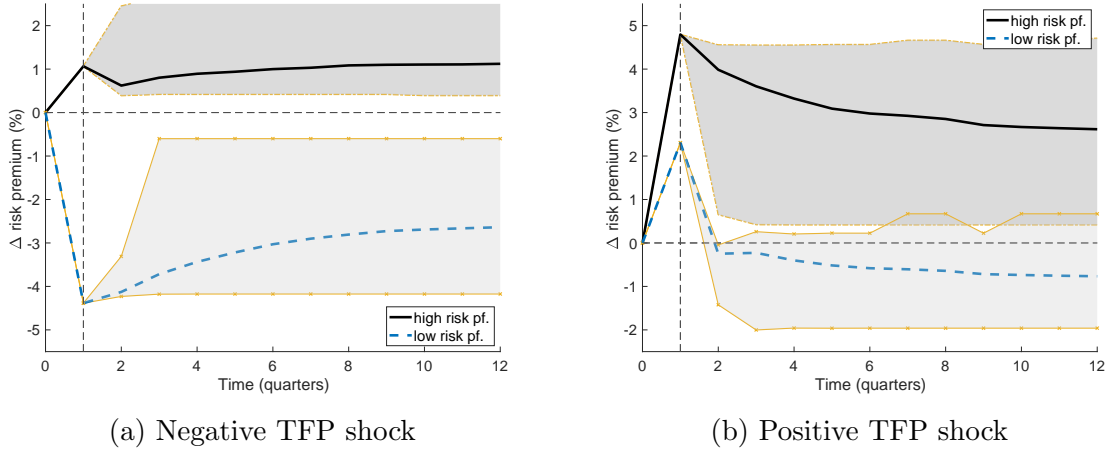

(a) Negative TFP shock   (b) Positive TFP shock

Figure 11: State-dependent risk premium dynamics

Notes: The figure plots the GTFs of the risk premium for a negative (panel (a)) and positive (panel (b)) 2% TFP shocks. The solid line represents the economy with the highest portion of risky asset before the shock hits and the dashed line does it for the economy with the lowest portion of risky asset.

constrained state (flight to safety). In contrast, when the economy begins with high risk exposure (solid black line), the risk premium spikes upward because the shock makes borrowing-constrained households immediately sell off their risky assets, pushing down contemporaneous risky asset prices and raising their expected return, increasing the risk premium. The key mechanism in distinctive patterns is in the constrained (wealth-poor) households' risk-free asset adjustment, which barely happens for the economy with high risk exposure, as they are already highly constrained.

Following a positive TFP shock (panel (b)), the pattern reverses. Economies with high pre-shock risky asset exposure experience a sharp drop in the risk premium, as improved prospects reduce precautionary motives and increase demand for risky assets. In contrast,

economies with low pre-shock risk exposure exhibit a modest increase in the premium, reflecting a financially less constrained economic state that does not have to rely largely on leveraging. Across all the scenarios, the responses are highly asymmetric and persistent, underscoring the importance of portfolio composition as a state variable in determining the dynamics of the risk premium. Notably, Figure 9 and Figure 10 show that the endogenous fluctuations in the portfolio are driven by the wealth-poor households. It reveals that the risk premium's state dependence crucially hinges on the wealth-poor households' existing wealth portfolio.

7   Concluding remarks

This paper develops a powerful global nonlinear solution framework in sequence space for solving dynamic stochastic general equilibrium models that achieves both global accuracy and computational efficiency without assuming perfect foresight. The framework also provides precise conditions under which sufficient statistics deliver exact solutions in models with complex aggregate states.

Next, I introduce the generalized transition function (GTF) as a subpath of the recursive competitive equilibrium (RCE). The GTF enables global nonlinear analysis including generalized impulse responses and stochastic growth paths within an integrated RCE framework. Moreover, it opens door to relatively overlooked important macroeconomic channels such as interplay between growth and uncertainty and the state dependent shock/policy sensitivities of economic variables.

Through the leading applications, I demonstrate the practical value of these frameworks, and I analyze novel model predictions: An economy becomes particularly fragile to a negative aggregate shock during the time of high hand-to-mouth household portion. Aggregate uncertainty substantially hampers capital stock growth in the short run. The fiscal multipliers are endogenous-state-dependent in the RCE. The rich and poor households display significantly different portfolio choices over the business cycle, while the latter becoming pro-active and taking more risk-loving stance. Moreover, the risk premium dynamics is substantially state-dependent: depending on the existing distribution of the wealth-poor households' wealth portfolio, the sign of its response to a TFP shock can flip. These are novel findings which became feasible due to the novel methodological advance this paper develops. This capability opens new possibilities for investigating complex nonlinear economic relationships and policy effects in modern macroeconomic models.

40

References

Ahn, S., G. Kaplan, B. Moll, T. Winberry, and C. Wolf (2018). When Inequality Matters for Macro and Macro Matters for Inequality. *NBER Macroeconomics Annual 32*, 1–75. _eprint: https://doi.org/10.1086/696046.

Aiyagari, S. R. (1994). Uninsured Idiosyncratic Risk and Aggregate Saving. *The Quarterly Journal of Economics 109*(3), 659–684. Publisher: Oxford University Press.

Algan, Y., O. Allais, and W. J. Den Haan (2008). Solving heterogeneous-agent models with parameterized cross-sectional distributions. *Journal of Economic Dynamics and Control 32*(3), 875–908.

Algan, Y., O. Allais, and W. J. Den Haan (2010). Solving the incomplete markets model with aggregate uncertainty using parameterized cross-sectional distributions. *Journal of Economic Dynamics and Control 34*(1), 59–68. Computational Suite of Models with Heterogeneous Agents: Incomplete Markets and Aggregate Uncertainty.

Alvarez, F., H. Le Bihan, and F. Lippi (2016, October). The real effects of monetary shocks in sticky price models: A sufficient statistic approach. *American Economic Review 106*(10), 2817–51.

Andreasen, M. M., J. Fernández-Villaverde, and J. F. Rubio-Ramírez (2017, 06). The pruned state-space system for non-linear dsge models: Theory and empirical applications. *The Review of Economic Studies 85*(1), 1–49.

Auclert, A., B. Bardóczy, M. Rognlie, and L. Straub (2021). Using the sequence-space jacobian to solve and estimate heterogeneous-agent models. *Econometrica 89*(5), 2375–2408.

Auclert, A., M. Rognlie, and L. Straub (2024). Fiscal and Monetary Policy with Heterogeneous Agents. *Working Paper*.

Auclert, A., M. Rognlie, L. Straub, and T. Tapak (2025). When Do Endogenous Portfolios Matter for HANK? *Working Paper*.

Bakota, I. (2023, October). Market Clearing and Krusell-Smith Algorithm in an Economy with Multiple Assets. *Computational Economics 62*(3), 1007–1045.

Baley, I. and A. Blanco (2021). Aggregate dynamics in lumpy economies. *Econometrica 89*(3), 1235–1264.

Basten, C., A. Fagereng, and K. Telle (2016). Saving and portfolio allocation before and after job loss. *Journal of Money, Credit and Banking 48*(2-3), 293–324.

Bayer, C. and R. Luetticke (2020). Solving discrete time heterogeneous agent models with aggregate risk and many idiosyncratic states by perturbation. *Quantitative Economics 11*(4), 1253–1288.

Bayer, C., R. Luetticke, L. Pham-Dao, and V. Tjaden (2019). Precautionary savings, illiquid assets, and the aggregate consequences of shocks to household income risk. *Econometrica 87*(1), 255–290.

Bhandari, A., T. Bourany, D. Evans, and M. Golosov (2023). A Perturbational Approach for Approximating Heterogeneous Agent Models. *Working Paper*.

Bloom, N., M. Floetotto, N. Jaimovich, I. Saporta-Eksten, and S. J. Terry (2018). Really Uncertain Business Cycles. *Econometrica 86*(3), 1031–1065.

Boppart, T., P. Krusell, and K. Mitman (2018, April). Exploiting MIT shocks in heterogeneous-agent economies: the impulse response as a numerical derivative. *Journal of Economic Dynamics and Control 89*, 68–92.

Cai, Y., K. Judd, and J. Steinbuks (2017, March). A nonlinear certainty equivalent approximation method for dynamic stochastic problems: Dynamic stochastic problems. *Quantitative Economics 8*(1), 117–147.

Calvet, L. E., J. Y. Campbell, and P. Sodini (2009, 02). Fight or flight? portfolio rebalancing by individual investors*. *The Quarterly Journal of Economics 124*(1), 301–348.

Cao, D. (2020). Recursive equilibrium in krusell and smith (1998). *Journal of Economic Theory 186*, 104978.

Cao, D., W. Luo, and G. Nie (2023, January). Global DSGE Models. *Review of Economic Dynamics*, S1094202523000017.

Childers, D. (2018). Solution of Rational Expectations Models with Function Valued States. *Working Paper*, 126.

Christiano, L., M. Eichenbaum, and S. Rebelo (2011). When is the government spending multiplier large? *Journal of Political Economy 119*(1), 78–121.

Christiano, L. J. and J. D. Fisher (2000). Algorithms for solving dynamic models with occasionally binding constraints. *Journal of Economic Dynamics and Control 24*(8), 1179–1232.

Cozzi, M. (2015, December). The Krusell–Smith Algorithm: Are Self-Fulfilling Equilibria Likely? *Computational Economics 46*(4), 653–670.

Den Haan, W. J. (1996). Heterogeneity, aggregate uncertainty, and the short-term interest rate. *Journal of Business & Economic Statistics 14*(4), 399–411.

Den Haan, W. J. (1997). Solving Dynamic Models with Aggregate Shocks and Heterogeneous Agents. *Macroeconomic Dynamics 1*(2), 355–386. Publisher: Cambridge University Press.

Den Haan, W. J. (2010, January). Assessing the accuracy of the aggregate law of motion in models with heterogeneous agents. *Journal of Economic Dynamics and Control 34*(1), 79–99.

Den Haan, W. J. and A. Marcet (1990). Solving the stochastic growth model by parameterizing expectations. *Journal of Business & Economic Statistics 8*(1), 31–34.

Den Haan, W. J. and P. Rendahl (2010, January). Solving the incomplete markets model with aggregate uncertainty using explicit aggregation. *Journal of Economic Dynamics and Control 34*(1), 69–78.

Elenev, V., T. Landvoigt, and S. Van Nieuwerburgh (2021). A Macroeconomic Model With Financially Constrained Producers and Intermediaries. *Econometrica 89*(3), 1361–1418.

Fagereng, A., C. Gottlieb, and L. Guiso (2017). Asset market participation and portfolio choice over the life-cycle. *The Journal of Finance 72*(2), 705–750.

Fagereng, A., L. Guiso, and L. Pistaferri (2017, 04). Portfolio choices, firm shocks, and uninsurable wage risk. *The Review of Economic Studies 85*(1), 437–474.

Fair, R. and J. Taylor (1983). Solution and Maximum Likelihood Estimation of Dynamic Nonlinear Rational Expectations Models. *Econometrica 51*(4), 1169–85.

Ferreira, M. H., T. Haber, and H. Lee (2025). The Inefficient Corporate Cash Buffer and the Nonlinear Business Cycle. *Working Paper*.

Ghassibe, M. and F. Zanetti (2022). State dependence of fiscal multipliers: the source of fluctuations matters. *Journal of Monetary Economics 132*, 1–23.

Gomes, F. and A. Michaelides (2007, 11). Asset pricing with limited risk sharing and heterogeneous agents. *The Review of Financial Studies 21*(1), 415–448.

Guerrieri, L. and M. Iacoviello (2015, March). OccBin: A toolkit for solving dynamic models with occasionally binding constraints easily. *Journal of Monetary Economics 70*, 22–38.

Hansen, L., J. Heaton, and N. Li (2008). Consumption strikes back? measuring long-run risk. *Journal of Political Economy 116*(2), 260–302.

Heaton, J. and D. Lucas (2000). Portfolio choice and asset prices: The importance of entrepreneurial risk. *The Journal of Finance 55*(3), 1163–1198.

Jo, Y. J. and S. Zubairy (2025, January). State-dependent government spending multipliers: Downward nominal wage rigidity and sources of business cycle fluctuations. *American Economic Journal: Macroeconomics 17*(1), 379–413.

Judd, K. L. (2002, August). The parametric path method: an alternative to Fair–Taylor and L–B–J for solving perfect foresight models. *Journal of Economic Dynamics and Control 26*(9-10), 1557–1583.

Judd, K. L., L. Maliar, and S. Maliar (2011, July). Numerically stable and accurate stochastic simulation approaches for solving dynamic economic models: Approaches for solving dynamic models. *Quantitative Economics 2*(2), 173–210.

Juillard, M. (1996). Dynare : a program for the resolution and simulation of dynamic models with forward variables through the use of a relaxation algorithm. *CEPREMAP Working Papers (Couverture Orange)* 9602, CEPREMAP.

Justiniano, A. and G. E. Primiceri (2008, June). The time-varying volatility of macroeconomic fluctuations. *American Economic Review 98*(3), 604–41.

Kahou, M. E., J. Fernandez-Villaverde, J. Perla, and A. Sood (2021). Exploiting Symmetry in High-Dimensional Dynamic Programming. *Working Paper*, 51.

Kaplan, G. and G. L. Violante (2014). A model of the consumption response to fiscal stimulus payments. *Econometrica 82*(4), 1199–1239.

Khan, A. and J. K. Thomas (2008, March). Idiosyncratic Shocks and the Role of Nonconvexities in Plant and Aggregate Investment Dynamics. *Econometrica 76*(2), 395–436.

Koop, G., M. Pesaran, and S. M. Potter (1996). Impulse response analysis in nonlinear multivariate models. *Journal of Econometrics 74*(1), 119–147.

Krusell, P. and A. A. Smith, Jr. (1997, June). Income and Wealth Heterogeneity, Portfolio Choice, and Equilibrium Asset Returns. *Macroeconomic Dynamics 1*(02).

Krusell, P. and A. A. Smith, Jr. (1998, October). Income and Wealth Heterogeneity in the Macroeconomy. *Journal of Political Economy 106*(5), 867–896.

Krusell, P. and A. A. Smith, Jr. (2006). Quantitative macroeconomic models with heterogeneous agents. *Econometric Society Monographs*.

Lee, H. and K. Nomura (2024). Global Nonlinear Equilibrium Dynamics and the Zero Lower Bound. *Working Paper*, 31.

Lee, H., P. Schnattinger, and F. Zanetti (2024). State-dependent Nonlinear Search and Matching. *Working Paper*, 31.

Luetticke, R. (2021, April). Transmission of monetary policy with heterogeneity in household portfolios. *American Economic Journal: Macroeconomics 13*(2), 1–25.

Maliar, L., S. Maliar, J. B. Taylor, and I. Tsener (2020). A tractable framework for analyzing a class of nonstationary Markov models. *Quantitative Economics 11*(4), 1289–1323.

Maliar, L., S. Maliar, and F. Valli (2010, January). Solving the incomplete markets model with aggregate uncertainty using the Krusell–Smith algorithm. *Journal of Economic Dynamics and Control 34*(1), 42–49.

Maliar, S., L. Maliar, and K. Judd (2011, February). Solving the multi-country real business cycle model using ergodic set methods. *Journal of Economic Dynamics and Control 35*(2), 207–228.

Marcet, A. (1988). Solving nonlinear stochastic models by parameterizing expectations. *Manuscript. Pittsburgh: Carnegie Mellon Univ.*

McGrattan, E. R. (1996). Solving the stochastic growth model with a finite element method. *Journal of Economic Dynamics and Control 20* (1), 19–42.

Meyn, S. P. and R. L. Tweedie (1993). *Markov Chains and Stochastic Stability*. Springer London.

Michaillat, P. (2014, January). A theory of countercyclical government multiplier. *American Economic Journal: Macroeconomics 6* (1), 190–217.

Petrosky-Nadeau, N., L. Zhang, and L.-A. Kuehn (2018, August). Endogenous disasters. *American Economic Review 108* (8), 2212–45.

Pizzinelli, C., K. Theodoridis, and F. Zanetti (2020). State dependence in labor market fluctuations. *International Economic Review 61* (3), 1027–1072.

Reiter, M. (2001, April). Recursive Solution Of Heterogeneous Agent Models. Computing in Economics and Finance 2001 167, Society for Computational Economics.

Reiter, M. (2009, March). Solving heterogeneous-agent models by projection and perturbation. *Journal of Economic Dynamics and Control 33* (3), 649–665.

Reiter, M. (2010). Solving the incomplete markets model with aggregate uncertainty by backward induction. *Journal of Economic Dynamics and Control 34* (1), 28–35. Computational Suite of Models with Heterogeneous Agents: Incomplete Markets and Aggregate Uncertainty.

Shen, W. and S.-C. S. Yang (2018). Downward nominal wage rigidity and state-dependent government spending multipliers. *Journal of Monetary Economics 98*, 11–26.

Spearman, C. (1904). The proof and measurement of association between two things. *The American Journal of Psychology 15* (1), 72–101.

Stokey, N. L., R. E. Lucas, and E. C. Prescott (1989). *Recursive Methods in Economic Dynamics*. Harvard University Press.

Winberry, T. (2018). A method for solving and estimating heterogeneous agent macro models. *Quantitative Economics 9* (3), 1123–1151.

Wright, B. D. and J. C. Williams (1982). The economic role of commodity storage. *The Economic Journal 92* (367), 596–614.

Wright, B. D. and J. C. Williams (1984). The welfare effects of the introduction of storage. *The Quarterly Journal of Economics 99* (1), 169–192.